Published December 9, 2013

Chemotherapy activates cancer-associated fibroblasts to maintain colorectal cancer-initiating cells by IL-17A

Fiorenza Lotti,[1] Awad M. Jarrar,[4] Rish K. Pai,[5] Masahiro Hitomi,[2,6] Justin Lathia,[1,2,6,9] Adam Mace,[4] Gerald A. Gantt Jr.,[4] Kumar Sukhdeo,[1] Jennifer DeVecchio,[1] Amit Vasanji,[7] Patrick Leahy,[8] Anita B. Hjelmeland,[1] Matthew F. Kalady,[1,3,4,6] and Jeremy N. Rich[1,6,9]

[1]Department of Stem Cell Biology and Regenerative Medicine, [2]Department of Cellular and Molecular Medicine, and [3]Department of Cancer Biology, Lerner Research Institute; [4]Department of Colorectal Surgery, Digestive Disease Institute; [5]Department of Anatomical Pathology, Pathology and Laboratory Medicine Institute, Cleveland Clinic, Cleveland, OH 44195
[6]Department of Molecular Medicine, Cleveland Clinic Lerner College of Medicine of Case Western Reserve University, Cleveland, OH 44195
[7]ImageIQ, Cleveland, OH 44106
[8]Department of General Medical Sciences–Oncology, Case Comprehensive Cancer Center, Case Western Reserve University, Cleveland, OH 44106
[9]National Center for Regenerative Medicine, Cleveland, OH 44106

Many solid cancers display cellular hierarchies with self-renewing, tumorigenic stemlike cells, or cancer-initiating cells (CICs) at the apex. Whereas CICs often exhibit relative resistance to conventional cancer therapies, they also receive critical maintenance cues from supportive stromal elements that also respond to cytotoxic therapies. To interrogate the interplay between chemotherapy and CICs, we investigated cellular heterogeneity in human colorectal cancers. Colorectal CICs were resistant to conventional chemotherapy in cell-autonomous assays, but CIC chemoresistance was also increased by cancer-associated fibroblasts (CAFs). Comparative analysis of matched colorectal cancer specimens from patients before and after cytotoxic treatment revealed a significant increase in CAFs. Chemotherapy-treated human CAFs promoted CIC self-renewal and in vivo tumor growth associated with increased secretion of specific cytokines and chemokines, including interleukin-17A (IL-17A). Exogenous IL-17A increased CIC self-renewal and invasion, and targeting IL-17A signaling impaired CIC growth. Notably, IL-17A was overexpressed by colorectal CAFs in response to chemotherapy with expression validated directly in patient-derived specimens without culture. These data suggest that chemotherapy induces remodeling of the tumor microenvironment to support the tumor cellular hierarchy through secreted factors. Incorporating simultaneous disruption of CIC mechanisms and interplay with the tumor microenvironment could optimize therapeutic targeting of cancer.

CORRESPONDENCE
Jeremy Rich:
drjeremyrich@gmail.com
OR
Matthew F. Kalady:
kaladym@ccf.org

Abbreviations used: CAF, cancer associated fibroblast; CIC, cancer initiating cell; HGF, hepatocyte growth factor.

Colorectal cancer is the third leading cause of cancer-related death in the United States, with ~141,210 new cases and 49,380 deaths in 2011 (American Cancer Society, 2011). Despite clinical advances, 50% of stage III and 95% of stage IV colorectal cancer patients will die from their disease (American Cancer Society, 2011). Improving survival for patients afflicted with colorectal cancer will require more effective and durable responses to adjuvant chemotherapy. Advances in the genetics of colorectal cancers have defined molecular targets altered during the development and progression of colorectal cancers, but have translated into targeted therapeutics with only modest efficacy. Tumor suppressor pathways account for most common genetic lesions, but these have proven difficult to target pharmacologically. Molecularly targeted therapies, like the anti–epidermal growth

F. Lotti and A.M. Jarrar contributed equally to this paper.

The Rockefeller University Press $30.00
J. Exp. Med. 2013 Vol. 210 No. 13 2851-2872
www.jem.org/cgi/doi/10.1084/jem.20131195

Supplemental Material can be found at:
/content/suppl/2013/12/04/jem.20131195.DC1.html

Published December 9, 2013

factor receptor (EGFR) agents cetuximab and panitumumab augment the activity of conventional chemotherapy but are not curative (Arnold and Seufferlein, 2010). Resistance to chemotherapy may be associated with the outgrowth of clones harboring advantageous genetic lesions, but cellular diversity derived from nongenetic sources also contributes to recurrent tumor growth (Weaver et al., 2002; Matsunaga et al., 2003; Bissell and Labarge, 2005). Cancers exist as complex systems composed of multiple cell types that collectively support and maintain tumor growth. Nontransformed elements may display relatively few genomic lesions and be more likely to display sustained responses to therapy, suggesting advantages to their use as therapeutic targets (Shaked et al., 2006, 2008; Yamauchi et al., 2008; Gilbert and Hemann., 2010; Hao et al., 2011; Shree et al., 2011; Straussman et al., 2012; Gilbert and Hemann., 2011; Acharyya et al., 2012; Nakasone et al., 2012; Hölzel et al., 2013; Bruchard et al., 2013). Indeed, the microenvironment has become a major focus in modeling the growth of cancer and therapeutic response. Inhibition of tumor vasculature through blockade of endothelial proliferation signals has clinical benefit, leading to the development of bevacizumab, a humanized anti–vascular endothelial growth factor (VEGF) antibody (Winder and Lenz, 2010). Another important compartment of tumor stroma is cancer-associated fibroblasts (CAFs). CAFs originate from heterogeneous cell types, including bone marrow–derived progenitor cells, smooth muscle cells, preadipocytes, fibroblasts, and myofibroblasts (Orimo and Weinberg, 2007; Worthley et al., 2010; Gonda et al., 2010). CAFs support tumorigenesis by stimulating angiogenesis, cancer cell proliferation, and invasion (Gonda et al., 2010; Worthley et al., 2010). They are also an important player in therapeutic resistance (Crawford et al., 2009; Porter et al., 2012), and fibroblasts can serve as a source for cytokines released in the cancer-initiating cell (CIC) microenvironment (Vermeulen et al., 2010). Furthermore, irradiated CAFs have been previously reported to promote tumor growth in breast (Barcellos-Hoff and Ravani, 2000) and lung cancers (Hellevik et al., 2013). It is thus logical that disruption of CAFs in the tumor microenvironment would influence clinical tumor behavior.

Cancers are maintained over the long term by a subpopulation of cancer cells, the CICs (Barker et al., 2009; Ricci-Vitiani et al., 2009; Blanpain, 2013). Like tissue-specific stem cells, the identification and characterization of CICs is evolving: the current definition is based on functional assays focused on recapitulation of the parental tumor upon xenotransplantation. The features of self-renewal, differentiation, and sustained proliferation are inherent within the regeneration of the tumor organ system (Magee et al., 2012). Interpatient variation in the genetics and epigenetics of colorectal cancers is so divergent that no identical mutational signatures have been reported for patients (Sanchez et al., 2009; Ogino et al., 2012; Sadanandam et al., 2013). It is therefore not surprising that markers to distinguish CICs from more differentiated progeny have not been absolutely informative across all tumors. Further, most CIC enrichment markers mediate interactions between a cell and its microenvironment, suggesting that the information associated with that marker may be lost after removal from the tumor microenvironment. Whereas CD133 (Prominin-1) had been reported by some groups to selectively identify colorectal CICs (O'Brien et al., 2007; Ricci-Vitiani et al., 2007; Elsaba et al., 2010; Fang et al., 2010), Shmelkov et al. (2008) reported that CD133 failed to inform identification of the CICs. Other groups have reported that CD44 (Dalerba et al., 2007; Du et al., 2008; Yeung et al., 2010; Ohata et al., 2012), CD166 (Dalerba et al., 2007; Vermeulen et al., 2008), CD66c (Gemei et al., 2013), Lgr5 (Barker et al., 2007; Vermeulen et al., 2008; Takahashi et al., 2011), or aldehyde dehydrogenase (ALDH; Huang et al., 2009; Deng et al., 2010) inform CIC characteristics. Regardless of the marker used, CICs are enriched for tumorigenic potential, indicating that these subgroups of tumor cells drive colorectal cancer maintenance and must be targeted to inhibit tumor growth.

CICs do not exist in isolation, but rather reside in an interactive niche with multiple cell types, including fibroblasts (Vermeulen et al., 2010; Medema and Vermeulen, 2011), endothelial cells (Lu et al., 2013), and immune cells (Hölzel et al., 2013). Each component contributes to the overall function and maintenance of the tumor and has potential roles in CIC resistance and recurrence. Mechanisms driving CIC maintenance and resistance are still being defined, but cell–cell interactions mediated through numerous molecular mechanisms, including cytokines and chemokines, are critical (Todaro et al., 2007; Vermeulen et al., 2010; Li et al., 2012). Cytokines and chemokines have the capacity to function as both paracrine and autocrine factors, supporting these secreted molecules as ideal mediators of interactions between the cellular hierarchy and other tumor cellular components. Indeed, we have described IL-6 as a key cue derived from more differentiated tumor cells to maintain glioblastoma CICs, which express IL-6 receptors (Wang et al., 2009). Mesenchymal stem cells and tumor-associated macrophages secrete IL-6 and CXCL7 in breast cancer to stimulate CIC growth and dispersal (Liu et al., 2011). These interactions are reciprocal, as CICs create supportive niches for stroma through the recruitment of mesenchymal stem cells via IL-1 secretion. In return, mesenchymal stem cells secrete IL-6 and IL-8 to promote CIC maintenance (Li et al., 2012).

Here, we first confirm that chemotherapy preferentially targets non-CICs due to cell autonomous resistance of CICs, but furthermore uncover a novel negative impact of chemotherapy in the stimulation of CAFs to create a chemoresistant niche by releasing cytokines, including IL-17A, as a CIC maintenance factor. These results have important clinical implications as most chemosensitizing approaches focus on disrupting cell autonomous molecular mechanisms without consideration of the interplay with the microenvironment that may display differential molecular dependence and temporal course, suggesting more complex therapeutic paradigms may be required to improve patient outcomes.

Published December 9, 2013

RESULTS

Interrogating the cellular hierarchy in human colorectal cancers

Heterogeneity in tumors is derived from a combination of genetic and epigenetic variance. A subset of tumor cells within colorectal cancers may display stem-like features. These CICs are defined functionally through self-renewal and phenocopy the complex parental tumor on secondary growth. The use of cell surface markers to enrich or deplete CICs is essential to segregate tumorigenic and nontumorigenic cells to demonstrate a cellular hierarchy. As several markers have been reported to selectively identify colorectal CICs, we first interrogated the ability to enrich for CICs in colorectal cancer patient specimens using several of the previously reported candidates (CD166, CD133, ALDH activity, and CD44; Dalerba et al., 2007; O'Brien et al., 2007; Ricci-Vitiani et al., 2007; Du et al., 2008; Vermeulen et al., 2008; Shmelkov et al., 2008; Huang et al., 2009; Fang et al., 2010; Elsaba et al., 2010; Yeung et al., 2010; Deng et al., 2010; Ohata et al., 2012). To avoid selection effects of cell culture, we interrogated markers in acutely dissociated patient specimens derived from either primary tumors or metastases (Fig. 1 A). Some markers, such as CD166, were not consistently expressed across tumors (not depicted) in concordance with other studies, suggesting specificity for colorectal cancer subtypes (Horst et al., 2009; Park et al., 2012). CD133 and ALDH activity measured by the Aldefluor assay were detectable but did not specifically segregate the capacity to generate tumor spheres (a surrogate marker of self-renewal associated with increased tumor initiation; unpublished data) or tumor initiation. Notably, CD44 consistently enriched for self-renewing, tumorigenic neoplastic cells (i.e., CICs). CD44 identified a minority of tumor cells (Fig. 1 A) that overlapped with cells that expressed the epithelial marker, EpCAM (Fig. 1 B), validating an epithelial origin as well as Aldefluor activity (Fig. 1 C) and CD133 antigen expression (Fig. 1 D). $CD44^{high/+}$ cells also had elevated levels of putative CIC genes (Blache et al., 2004; Jay et al., 2005; Takahashi and Yamanaka, 2006; Huang et al., 2009; Deng et al., 2010; Guo et al., 2012), including c-Myc, ALDH1, Sox9, Oct4, Musashi1 (Msi1), and BMI1, when compared with $CD44^{low/-}$ cells (Fig. 1 E). These data indicate that $CD44^{high/+}$ colorectal cancer cells coexpress other CIC markers. The coexpression of CD44, EpCAM, Aldefluor, and CD133 was validated in four independent samples (Fig. 1 F). CD44 is a receptor for components of the extracellular matrix. Like most receptors, its expression is down-regulated in response to ligand engagement. To assess the difference of in vivo versus in vitro environmental effects on the fraction of $CD44^{high/+}$ cells, single cell suspensions from freshly dissociated patients' colorectal tumors and their cultured counterparts were analyzed by FACS for the expression of CD44. As expected, the fractions differed based on growth conditions, but a general concordance in the relative degree of $CD44^{high/+}$ fractions within each condition was observed (Fig. 1 G). The clinical characteristics of these samples are summarized in Table S1.

To further evaluate the ability of CD44 to enrich for CICs, we next examined key functional assays (tumorsphere formation and tumor propagation). Using several human colorectal cancer specimens from different sites (primary and metastatic), stages, and genetic backgrounds, we compared the phenotype of $CD44^{high/+}$ and $CD44^{low/-}$ cells. $CD44^{high/+}$ cells formed tumorspheres within 14 d at high efficiency compared with $CD44^{low/-}$ cells (Fig. 1 H). In a limiting dilution assay, $CD44^{high/+}$ showed a higher estimated stem cell forming frequency compared with $CD44^{low/-}$ (Fig. 1 I). When implanted into immunocompromised hosts, $CD44^{high/+}$ cells formed tumors that phenocopied the parental tumor (Fig. 1 J). 2×10^4 $CD44^{high/+}$ cells initiated tumors in at least 80% of immunocompromised mice injected from four different colorectal cancer patient specimens, whereas 2×10^5 $CD44^{low/-}$ cells were not sufficient to form tumors (Fig. 1 K). Collectively, these data suggest that CICs can be prospectively identified and characterized in the $CD44^{high/+}$ cell population, whereas non-CICs are $CD44^{low/-}$.

CICs display cell autonomous resistance to chemotherapy

The ability to prospectively enrich and deplete CICs permits comparative analysis of selected tumor cell phenotypes. Although therapeutic resistance is not a defining feature of CICs, relative chemoresistance has been reported for CICs (Lakshman et al., 2004, 2005; Todaro et al., 2007; Dylla et al., 2008; Dallas et al., 2009). We interrogated the responses of matched CICs and non-CICs derived from human colorectal carcinomas to a clinically relevant chemotherapy combination (FOLFOX: fluorouracil [5-FU], oxaliplatin, and leucovorin; Fig. 2). In two human tumor systems, the basal viability of CICs was similar to matched non-CICs (Fig. 2 A). Upon chemotherapy treatment, both CICs and non-CICs showed a decrease in relative viability, but CICs were significantly less sensitive to chemotherapy. To determine the cellular phenotype responsible for this change, we quantified apoptosis and found that basal apoptosis was relatively similar in CICs and non-CICs, but chemotherapy-induced apoptosis was significantly reduced in the CICs relative to non-CICs (Fig. 2 B). The relative resistance of CICs to chemotherapy suggests that CICs may be enriched after chemotherapy treatment. Indeed, the CIC immunophenotype ($CD44^{high/+}$) was increased 1.5–3-fold after chemotherapy treatment in 4 human tumor models (Fig. 2 C and not depicted). Collectively, these results support a cell-autonomous relative chemoresistant phenotype of colorectal CICs.

Tumor response to treatment is associated with increased frequency of CAFs

Prior studies have suggested that cytotoxic therapy alters the stromal compartment in colorectal cancer (Washington et al., 2009; Edge et al., 2009), suggesting that this remodeling may be an extrinsic regulator of CICs. We therefore interrogated the stromal response in a cohort of colorectal patients treated with cytotoxic therapy. We investigated CAFs based on their proposed roles in supporting tumorigenesis (Olumi et al.,

Published December 9, 2013

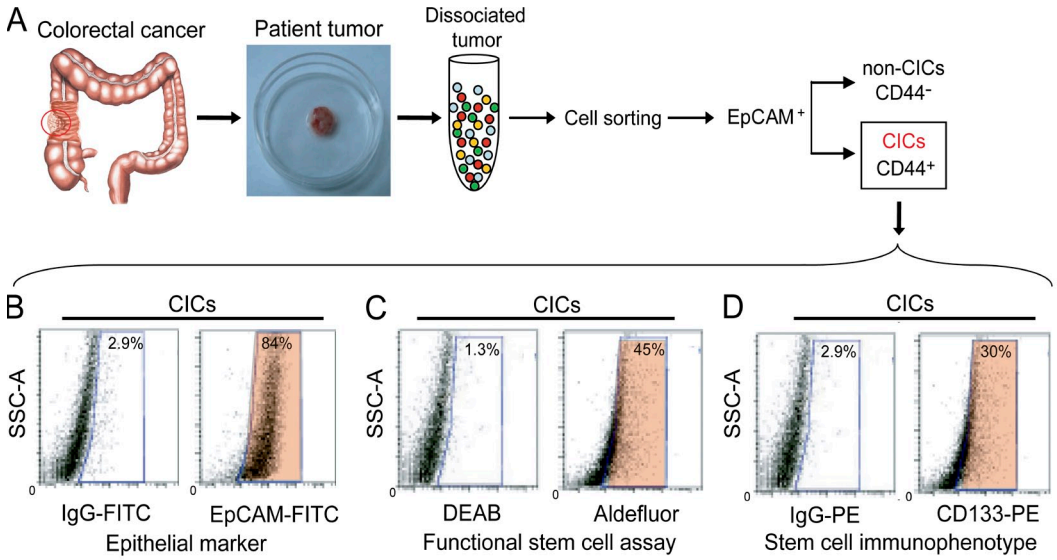

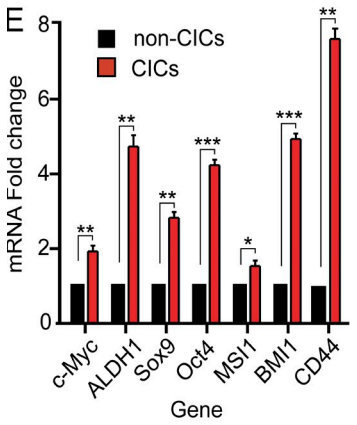

F

Tumor	CD44+ (%)	EpCAM (%)	Aldefluor	CD133 (%)
064	6.3	84	45	30
199	4.5	91	31	28
656	7.2	95	37	21
586	4.1	87	56	22

G

Tumor	CD44+ *in vivo* (%)	CD44+ *in vitro* (%)
064	6.3	25
199	4.5	10
656	7.2	21
586	4.1	8

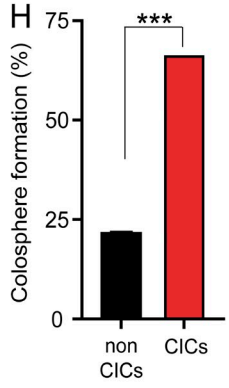

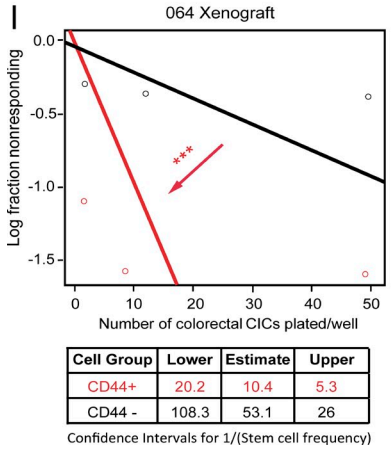

Cell Group	Lower	Estimate	Upper
CD44+	20.2	10.4	5.3
CD44 -	108.3	53.1	26

Confidence Intervals for 1/(Stem cell frequency)

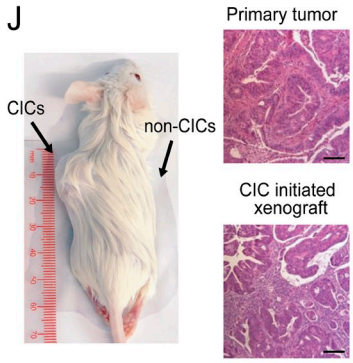

K

Tumor	Source	Group	# Cells	# Tumors
064	Xenograft	CICs	$2x10^4$	5/5
		non-CICs	$2x10^5$	0/5
		Bulk	$2x10^5$	3/5
199	Xenograft	CICs	$2x10^4$	4/5
		non-CICs	$2x10^5$	0/5
		Bulk	$2x10^5$	2/5
656	Xenograft	CICs	$2x10^4$	5/5
		non-CICs	$2x10^5$	0/5
		Bulk	$2x10^5$	3/5
586	Xenograft	CICs	$2x10^4$	4/5
		non-CICs	$2x10^5$	0/5
		Bulk	$2x10^5$	3/5

Tumorigenicity of Colon Cancer Cells

Figure 1. CD44 identifies CICs. (A) Single-cell suspensions from dissociated patient colorectal tumors were sorted by FACS for high expression of CD44-PE. The highly positive population was gated in a range of 4 to 10% (depending on the percentage of the total positive cell population of each sample) of the tail of the positive cells. (B–D) CICs were analyzed by FACS: (B) the epithelial marker EpCAM-FITC; (C) the functional stem cell assay Aldefluor; and (D) the stem cell immunophenotype by CD133-PE. (E) Quantitative RT-PCR analysis of CIC markers including c-Myc, ALDH1, Sox9, Oct4, MSI1, BMI1, and CD44 was performed on CICs and non-CICs. Data are presented as mean ± SD ($n = 3$); *, $P < 0.05$; **, $P < 0.01$; ***, $P < 0.001$. Student's *t* test was used to assess the significance. The experiment was performed twice and representative data are shown. (F) Colorectal tumor specimens from patients were subjected to dissociation to single cells and FACS sorting for high expression of CD44. The frequency of $CD44^+$ in each tumor is indicated in the $CD44^+$ column of the table. $CD44^+$ cells were sequentially analyzed for the expression of the epithelial marker EpCAM, the functional stem cell assay

Published December 9, 2013

1999; Allinen et al., 2004; Orimo et al., 2005; Erez et al., 2010; Vermeulen et al., 2010; Calon et al., 2012). CAFs are not homogeneous, but rather display distinctive characteristics based on tumor type and stage (Micke and Ostman, 2004; Desmoulière et al., 2004; Sugimoto et al., 2006; Orimo and Weinberg, 2007; Xing et al., 2010). To model CAF evolution in colorectal cancer after cytotoxic treatment, we quantified CAFs during the course of therapy in human patients. In matched specimens from identical patients before and after cytotoxic treatment, we stained for CAF markers α-smooth muscle actin (αSMA) and vimentin (Sappino et al., 1988; Rønnov-Jessen et al., 1996; Serini and Gabbiani, 1999; De Wever and Mareel, 2002; Nakayama et al., 2002; Orimo and Weinberg, 2007; Worthley et al., 2010; Gonda et al., 2010). Immunohistochemistry demonstrated that fibroblast markers, including vimentin and αSMA, increased after treatment, whereas the epithelial marker EpCAM decreased (Fig. 3 A). Quantitative measures of the relative proportion of fibroblasts to the epithelial component (αSMA versus EpCAM) further demonstrated that CAFs were significantly increased after treatment (Fig. 3 B). We validated these findings using transcriptional profiling on a larger cohort of samples derived from patients who were either untreated or treated with cytotoxic regimens (17 samples each group; Fig. 3 C). These results confirm that CAFs are enriched during post-therapy tumor growth. Clinical characteristics and treatment data for the cohort of patients used above are summarized in Tables S2 and S3.

As shown in our findings and in previous studies (Dallas et al., 2009; Dylla et al., 2008; Lakshman et al., 2004; Lakshman et al., 2005; Todaro et al., 2007), CICs display cell autonomous therapeutic resistance, but the significant increase in the percentage of CAFs after cytotoxic treatment suggests that treatment may also induce the remodeling of the tumor microenvironment and CAFs may provide microenvironmental cues instructing the cellular hierarchy. A previous study demonstrated that an immortalized colon fibroblast cell line derived from normal colon increases CIC proliferation (Vermeulen et al., 2010). To extend these findings to human CAFs, we prospectively isolated viable CAFs from freshly resected patient colorectal cancer specimens using the cell surface protein, platelet-derived growth factor receptor α (PDGFRα; Erez et al., 2010; Micke and Ostman, 2004; Fig. 3 D). We then confirmed the cell immunophenotype via immunofluorescence of multiple activated fibroblast markers, such as PDGFRα, vimentin, αSMA, FAP (Park et al., 1999; Calon et al., 2012), and FSP1 (Grum-Schwensen et al., 2005; Sugimoto et al., 2006); we also confirmed the absence of the epithelial marker EpCAM (Fig. 3 E), the smooth muscle marker smoothelin (Gonda et al., 2010), and the pericyte marker high molecular weight caldesmon (Nakayama et al., 2002; not depicted). These patient-derived CAF cultures expressed activated fibroblast lineage markers without significant contamination by epithelial cells.

Chemotherapy-stimulated CAFs promote CIC growth

To determine the impact of CAFs on CICs, we performed a series of co-culture studies with the two cell types in proximity but not in direct contact. Both CICs and non-CICs had modest increases in cell viability when co-cultured with CAFs, demonstrating a general effect of CAFs in promoting tumor growth (unpublished data). However, co-culture of chemotherapy-treated CAFs increased the viability of CICs compared with vehicle-treated control CAFs (Fig. 4 A). As CAFs are phenotypically distinct from normal tissue fibroblasts and systemically administered chemotherapy induces genotoxic stress tissue-wide to create selection pressure in microenvironmental elements, prior studies may underestimate the role of CAFs in therapeutic resistance and recurrent tumor growth. In support of this hypothesis, we found that even normal fibroblasts (i.e., not CAFs) treated with chemotherapy increased CIC viability relative to untreated fibroblasts (Fig. 4 A). As cell–cell interactions such as those between CICs and CAFs can be mediated through paracrine factors that regulate the tumor hierarchy, we hypothesized that chemotherapy-induced CAFs secrete factors to maintain CICs. Indeed, we found that conditioned media from CAFs mimicked the effects of CAF co-culture on CIC growth (Fig. 4 B).

To determine the effects of CAFs on in vivo tumor growth, we implanted 3,000 CICs alone or in combination with CAFs pretreated with chemotherapy or vehicle control. In concordance with cell culture results, chemotherapy activation of CAFs augmented the ability of CICs to initiate tumors in immunocompromised mice (Fig. 4 C). The presence of CAFs increased tumor incidence and reduced the latency of tumor formation by CICs with increased tumor size in

Aldefluor, and the stem cell immunophenotype CD133. The percentages of marker positive $CD44^+$ cells obtained are listed in a tabular form. (G) Single-cell suspensions from dissociated patient colorectal tumors and cells cultured in stem cell medium were analyzed by FACS for the expression of CD44. The percentages obtained are listed in a tabular form. (H) Quantification of sphere-formation assay demonstrates that CICs have elevated tumorsphere formation efficiency. CICs and non-CICs from two samples were plated in 96-well plates for a period of 14 d. Data are presented as a percentage of wells containing tumorspheres compared to the total number of wells. Data are presented as mean ± SD (n = 2); ***, $P < 0.001$. Student's t test was used to assess the significance. The experiment was performed two times and representative data are shown. (I) Limiting dilution assay demonstrates that $CD44^+$ cells have elevated tumorsphere formation efficiency. $CD44^+$ and $CD44^-$ population from two samples were plated in limiting dilution (50, 10, 1 cell[s] per well) in 96-well plates in stem cell media. The presence of spheres was evaluated after 14 d. Data are presented as mean ± SD ($n = 20$); ***, $P < 0.001$. The likelihood ratio test was used to assess the significance. The experiment was performed two times and representative data are shown. (J) Representative images of tumors initiated from CICs subcutaneously implanted into immunocompromised mice with hematoxylin and eosin staining of tumor sections. Scale bar, 100 μm. (K) CICs were tumorigenic while 10 fold more non-CICs were unable to generate tumors in four independent specimens. Five mice were used per group.

Published December 9, 2013

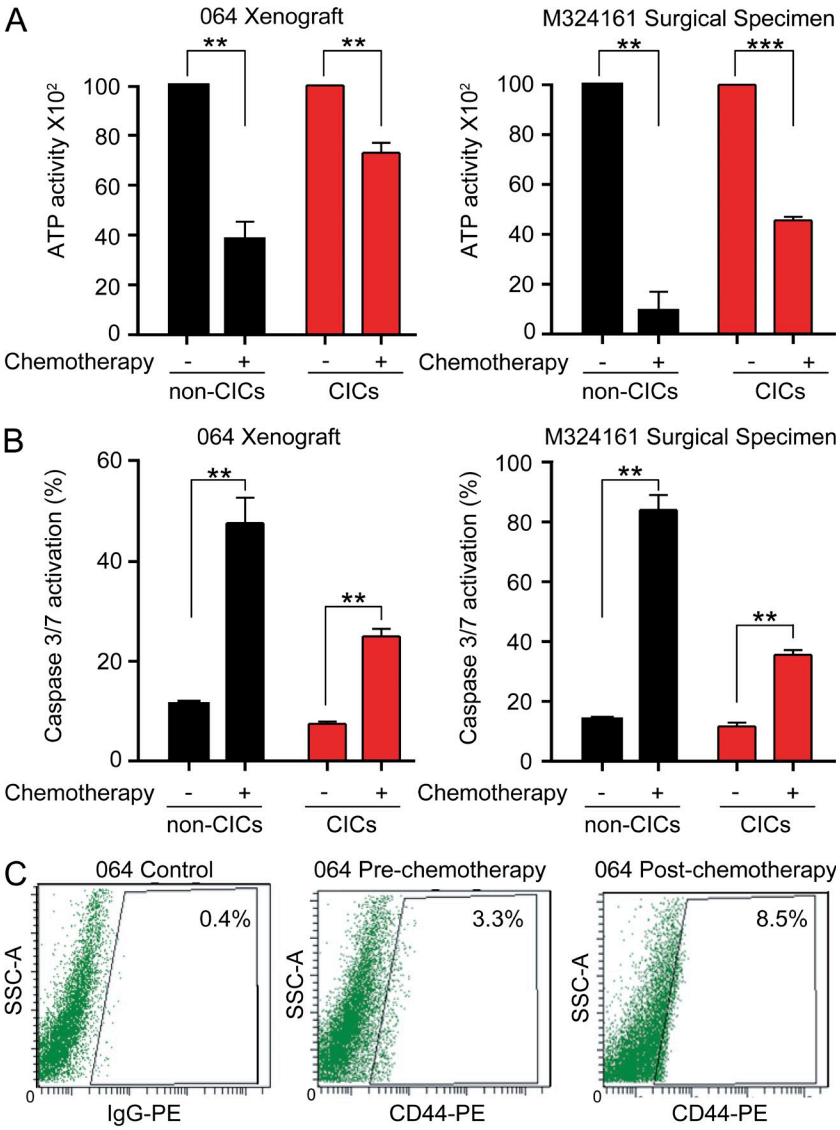

Tumor	Source	CD44 pre-chemotherapy (%)	CD44 post-chemotherapy (%)
064	Xenograft	3.3	8.5
M324161	Patient	2.5	7.0
M3124184	Patient	4.1	6.4
M3124336	Patient	2.2	6.8

Figure 2. Tumor response to treatment is associated with increased frequency and resistance of CICs. (A) Cell growth of CICs and non-CICs from two independent human specimens was assessed by ATP based assay (CellTiter-Glo) following chemotherapy (FOLFOX: 50 µg/ml 5-flurouracil + 10 µM oxaliplatin + 1 µM leucovorin). Data are presented as mean ± SD (n = 3); **, $P < 0.01$; ***, $P < 0.001$. Student's *t* test was used to assess the significance. The experiment was performed three times and representative data are shown. (B) Apoptosis of CICs and non-CICs from two independent human specimens was assessed by caspase 3/7 activation after chemotherapy. Data are presented as mean ± SD ($n = 3$); **, $P < 0.01$. Student's *t* test was used to assess the significance. The experiment was performed three times and representative data are shown. (C) Enrichment of CICs in bulk cells from four independent human specimens was assessed by FACS analysis for CD44 (representative sample) after chemotherapy. Student's *t* test was used to assess the significance. The experiment was performed once for each individual specimen.

mice co-implanted with CICs and chemotherapy-pretreated CAFs (Fig. 4 C). Moreover, xenografts generated by CICs co-implanted with chemotherapy-treated CAFs displayed increased proliferative indices (Fig. 4 D) and the CIC immunophenotype (percentage of $CD44^{high/+}$ cells by FACS analysis; Fig. 4 E). To establish the effects on CICs in functional assays, we performed secondary in vitro tumorsphere formation assays (Fig. 4 F) and measurement of resistance to cytotoxic treatment (ATP activity; Fig. 4 G) finding induction of increased cell survival and growth with chemotherapy-treated CAFs compared with the effects of untreated CAFs, suggesting specific effects on CIC maintenance. These data collectively support a model in which chemotherapy activates CAFs in the microenvironment to stimulate CIC growth and stimulate tumor growth.

Chemotherapy stimulates CAF cytokine secretion

These data demonstrated the presence of biologically important components in CAF secretome, so we performed a comparative analysis of cytokine expression in conditioned media of CAFs at baseline or treated with chemotherapy in three different patient specimens, as well as in normal fibroblasts. Although there were several molecules unique to each CAF, there were only three common molecules to every

Published December 9, 2013

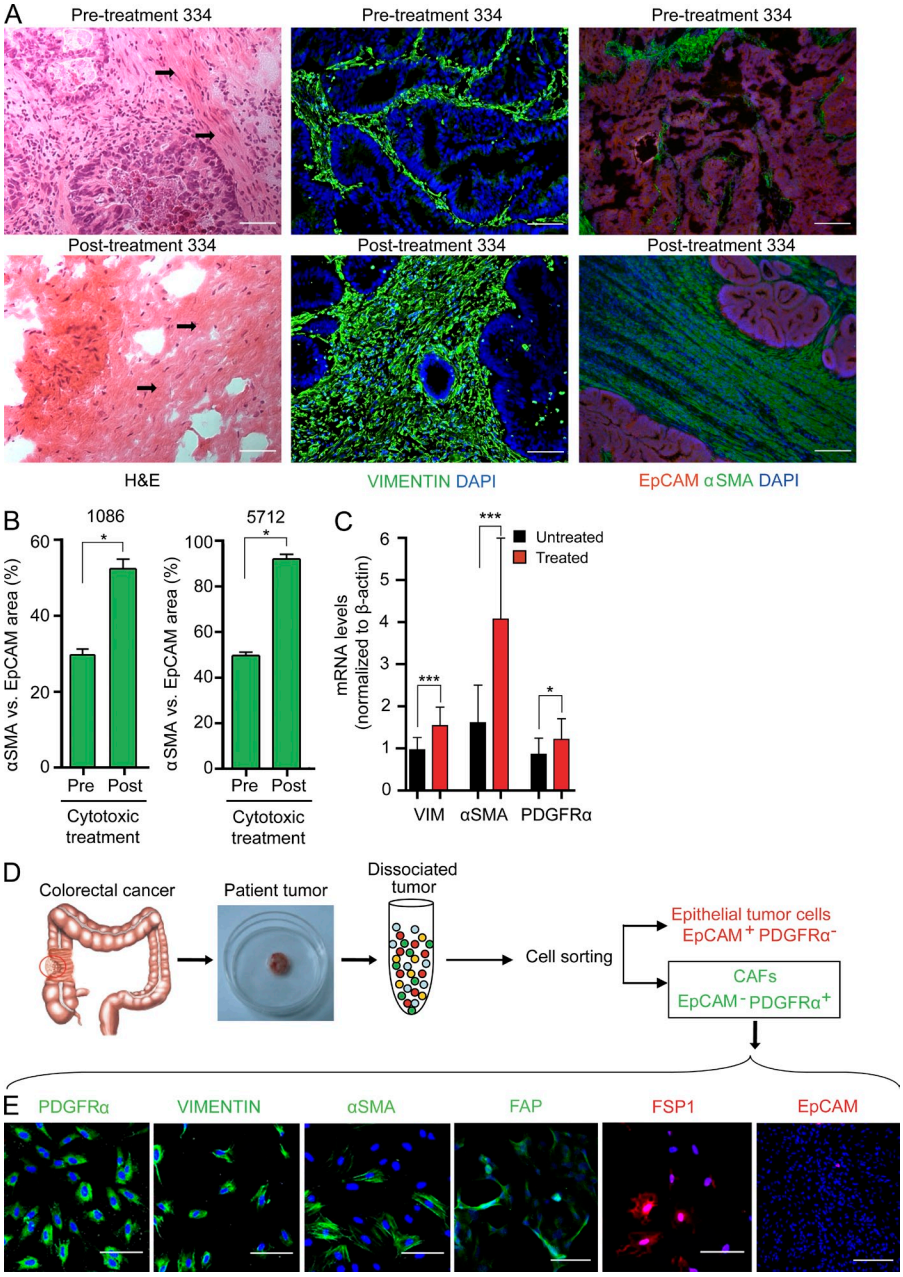

Figure 3. Tumor response to treatment is associated with increased frequency of CAFs. (A) Frozen sections of human colorectal tumors matched before and after cytotoxic treatment from a representative patient (334) were stained for markers of activated fibroblasts (Vimentin, αSMA) and epithelial cells (EpCAM). Nuclei stained with DAPI. Arrows indicate the stromal compartment. (B) Frozen sections of human colorectal tumors matched before and after cytotoxic treatment from two different patients (1086 or 5712) were stained for αSMA and EpCAM. The ratio of the αSMA-positive area versus the EpCAM-positive area was quantified and shown on the right. Data are presented as mean ± SD. *, $P < 0.05$. Student's *t* test was used to assess the significance. Data are representative of three experimental repeats per group. (C) cDNA levels of markers of activated fibroblasts (Vimentin, α-SMA, and PDGFRα) were quantified by quantitative RT-PCR in patients untreated and treated (17 samples each group). Data are presented as mean ± SD; *, $P < 0.05$; ***, $P < 0.001$. Student's *t* test was used to assess the significance. The experiment was performed three times and representative data are shown. (D) Single cell suspensions from dissociated patient colorectal tumor were sorted by FACS for the expression of PGDFRα-PE. The purity of the sorted population was checked after the sorting. (E) The PDGFRα+ isolated population was validated by positive immunostaining for CAF markers (αSMA-Vimentin-FSP1-FAP) and negative immunostaining for an epithelial marker (EpCAM). Bars: (A and E) 50 µm.

chemotherapy-induced CAF culture: the secreted DTK (TYRO3) receptor, IL-17A, and TGFβ (Fig. 5 A). A prior study suggested that a single normal, immortalized fibroblast line stimulated a CIC model through secretion of hepatocyte growth factor (HGF; Vermeulen et al., 2010). In our analysis, HGF was not significantly associated with chemotherapy response, suggesting that HGF may contribute to initial tumor growth but is less likely to be associated with chemotherapy response (Fig. 5 B). In contrast, sDTK, IL-17A, and TGFβ were expressed at low levels in quiescent tumor-derived and normal colon fibroblasts, but the expression of each molecule dramatically increased after chemotherapy in CAFs but not normal colon fibroblasts (Fig. 5 C). This regulation appeared to occur at the level of transcription, as similar increases were detectable for each target at the mRNA level (Fig. 5 D). Among the three top up-regulated cytokines (IL-17A, TGFβ, and GAS6 [DTK ligand]), TGFβ and GAS6 did not directly stimulate CIC growth (unpublished data) so we focused on IL-17A. CAF expression of IL-17A protein was further confirmed by immunofluorescence double staining of αSMA and IL-17A of matched human patient samples before and after cytotoxic treatment (Fig. 5 E).

To extend these observations to a clinical paradigm, we quantified IL-17A mRNA in cohorts of colorectal cancer tumor specimens from patients either untreated or treated (17 patients in each group; Fig. 6 A; clinical data are summarized

Published December 9, 2013

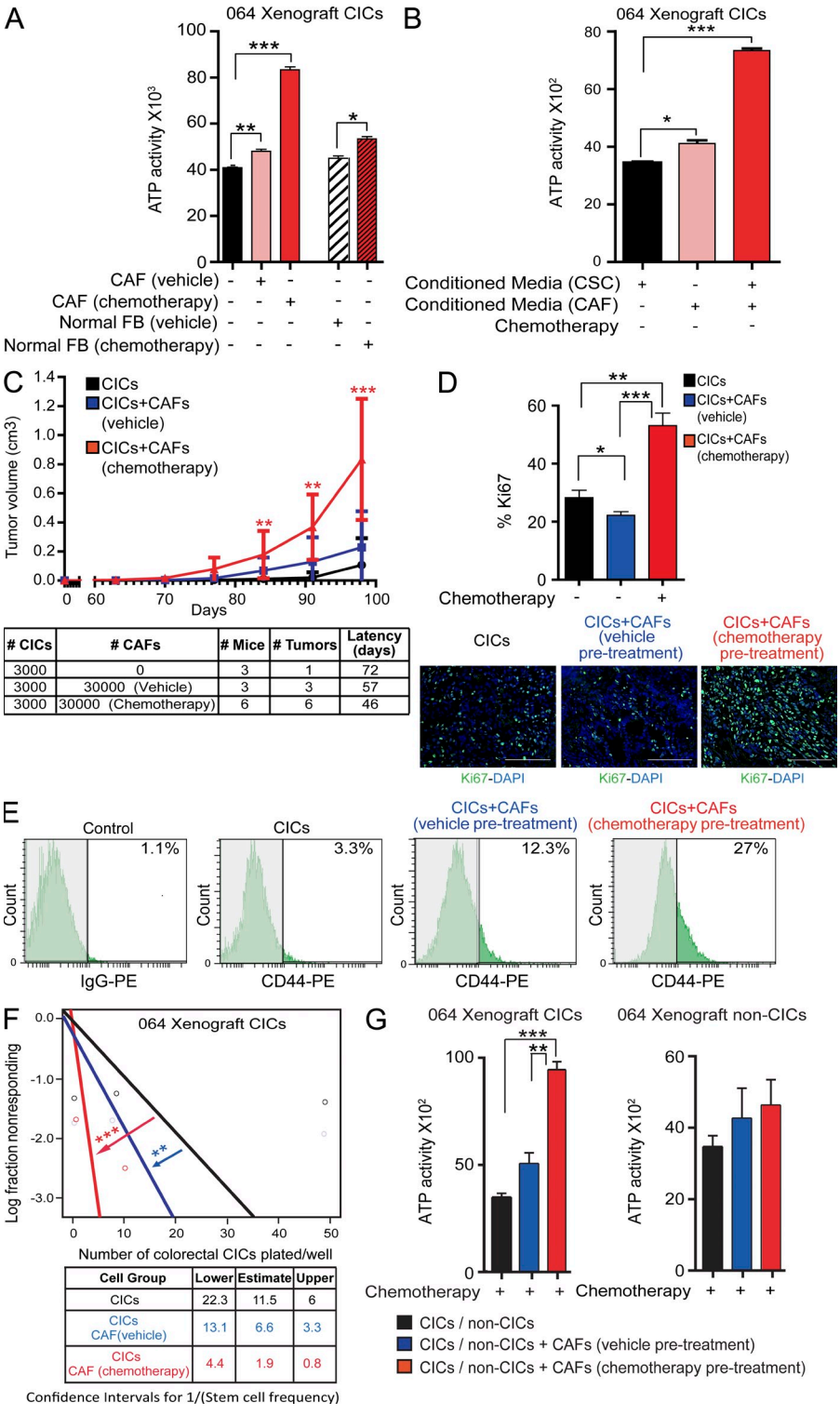

# CICs	# CAFs	# Mice	# Tumors	Latency (days)
3000	0	3	1	72
3000	30000 (Vehicle)	3	3	57
3000	30000 (Chemotherapy)	6	6	46

Cell Group	Lower	Estimate	Upper
CICs	22.3	11.5	6
CICs CAF(vehicle)	13.1	6.6	3.3
CICs CAF (chemotherapy)	4.4	1.9	0.8

Figure 4. Chemotherapy-stimulated CAFs promote CIC growth and chemoresistance. The effect of CAFs on CICs was assessed by (A) co-culture and (B) conditioned media treatment. (A) 10^4 CICs were cultured with 2×10^4 CAFs or normal fibroblasts treated with vehicle (DMSO) or chemotherapy for 10 d. Cellular viability was measured by Cell Titer-Glo assay. Data are presented as mean ± SD ($n = 3$); *, $P < 0.05$; **, $P < 0.01$; ***, $P < 0.001$. Student's t test was used to assess the significance. The experiment was performed three times and representative data are shown. (B) 1.5×10^5 CICs and CAFs were treated with vehicle (DMSO) or chemotherapy for 3 d. Conditioned media were collected and use to culture CICs for 10 d. Cellular viability was measured by Cell Titer-Glo assay. Data are presented as mean ± SD ($n = 3$); *, $P < 0.1$; ***, $P < 0.001$. Student's t-test was used to assess the significance. The experiment was performed three times and representative data are shown. (C) The ability of the CAFs to affect the tumorigenic capacity of CICs from two different human specimens was tested in vivo. 3×10^4 CAFs treated with vehicle (DMSO) or with chemotherapy for 3 d were subcutaneously co-implanted in immunocompromised mice with 3×10^3 CICs. Tumors were monitored every day to evaluate the latency, harvested simultaneously, and volume measured to evaluate their development. **, $P < 0.01$; ***, $P < 0.001$. ANOVA, followed by Bonferroni's post-hoc test was used to assess the significance. As indicated in the table, three to six mice were used in each group. The contribution of CAFs to post-therapy tumor growth was assessed by immunostaining of the xenografts for Ki-67 (D). Nuclei were counterstained with DAPI. Quantification was done by counting four high-power fields per condition. Data are presented as mean ± SD; *, $P < 0.05$; **, $P < 0.01$; ***, $P < 0.001$. Student's t-test was used to assess the significance. Bars, 50 µm. (E) Xenografts derived from data in C were dissociated and analyzed for the expression of CD44 by FACS. Colorectal cancer cells conditioned by the presence of the CAFs were enriched in the CD44 compartment. (F) CICs sorted from xenografts in C were plated in 96-well plates in limiting dilution (50, 10, or 1 cells per well) and analyzed for sphere formation. Data are presented as mean ± SD ($n = 20$); **, $P < 0.01$; ***, $P < 0.001$. The likelihood ratio test was used to assess the significance. The experiment was performed once. (G) 3×10^4 CICs and non-CICs from the same xenografts (C) were plated in 96-well plates and treated with chemotherapy. The effect of CAFs on CICs and non-CICs cells chemosensitivity was tested by evaluating cell viability (absolute number) measured by CellTiter-Glo assay. Data are mean ± SD ($n = 3$); **, $P < 0.01$; ***, $P < 0.001$; unlabeled, $P > 0.05$. Student's t test was used to assess the significance. The experiment was performed twice and representative data are shown.

Published December 9, 2013

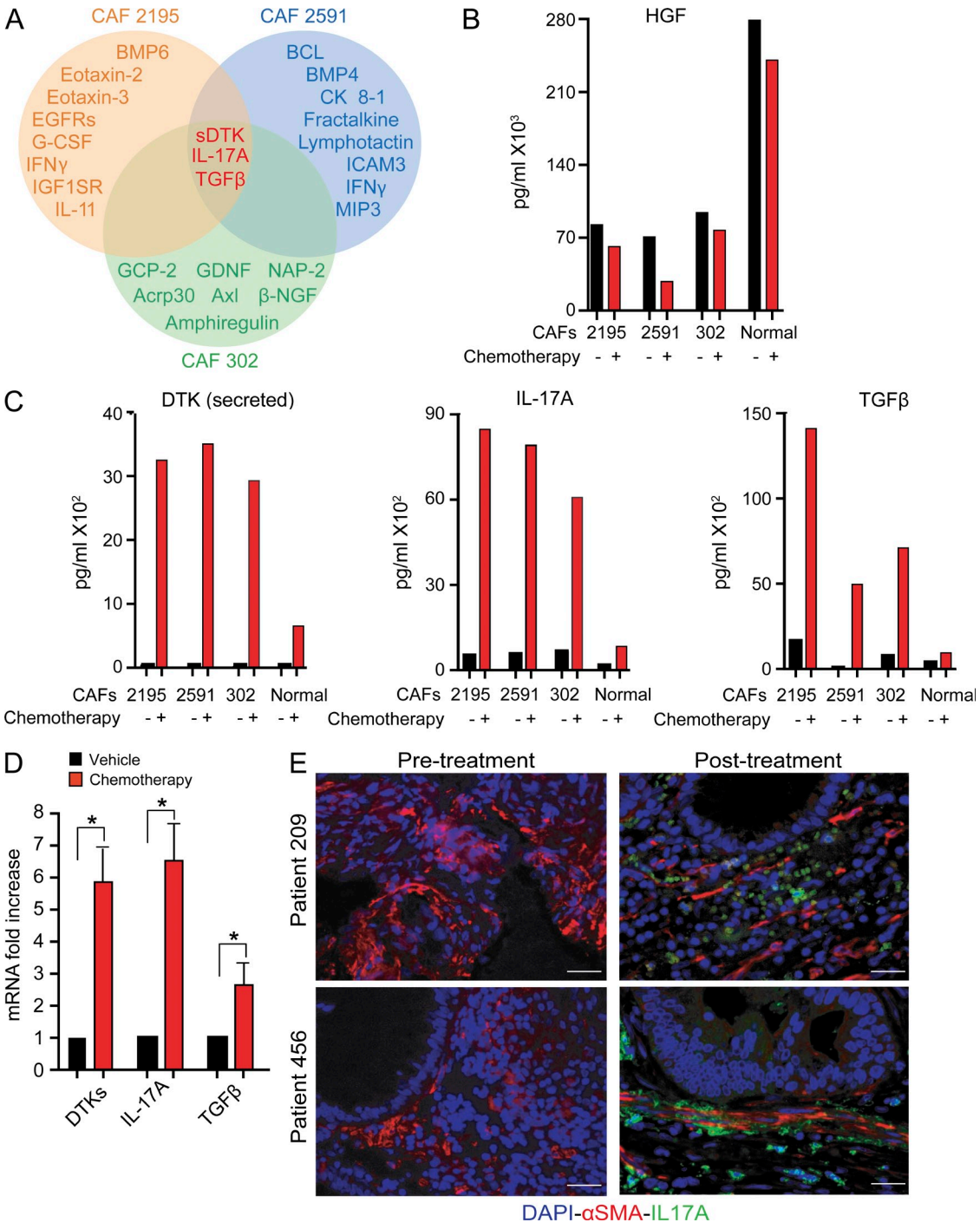

Figure 5. Chemotherapy stimulates CAF cytokine secretion. Cytokine secretion of CAFs treated with vehicle (DMSO) or with chemotherapy for 3 d was assessed using a 120 human cytokine antibody array from RayBio. (A–C) CAFs derived from three human surgical specimens and one commercial normal intestinal fibroblast line were interrogated for their cytokine and chemokine profile after chemotherapy treatment. (B) HGF was not significantly up-regulated in our cytotoxin conditions compared with vehicle. (C) The mean concentrations of DTK, IL-17A, and TGFβ were statistically significant in the three CAFs treated with chemotherapy compared with vehicle. ($n = 1$); $P < 0.05$. Student's t test was used to assess the significance. The experiment was performed once. (D) Quantitative RT-PCR analysis of DTKs, IL-17A, and TGFβ was performed to validate the cytokine array results. Data are presented as mean ± SD ($n = 3$); *, $P < 0.05$. Student's t test was used to assess the significance. The experiment was performed three times and representative data are shown. (E) Frozen sections of human colorectal tumors matched before and after cytotoxic treatment from two patients were co-stained for IL-17A and αSMA. Bars, 50 µm.

Published December 9, 2013

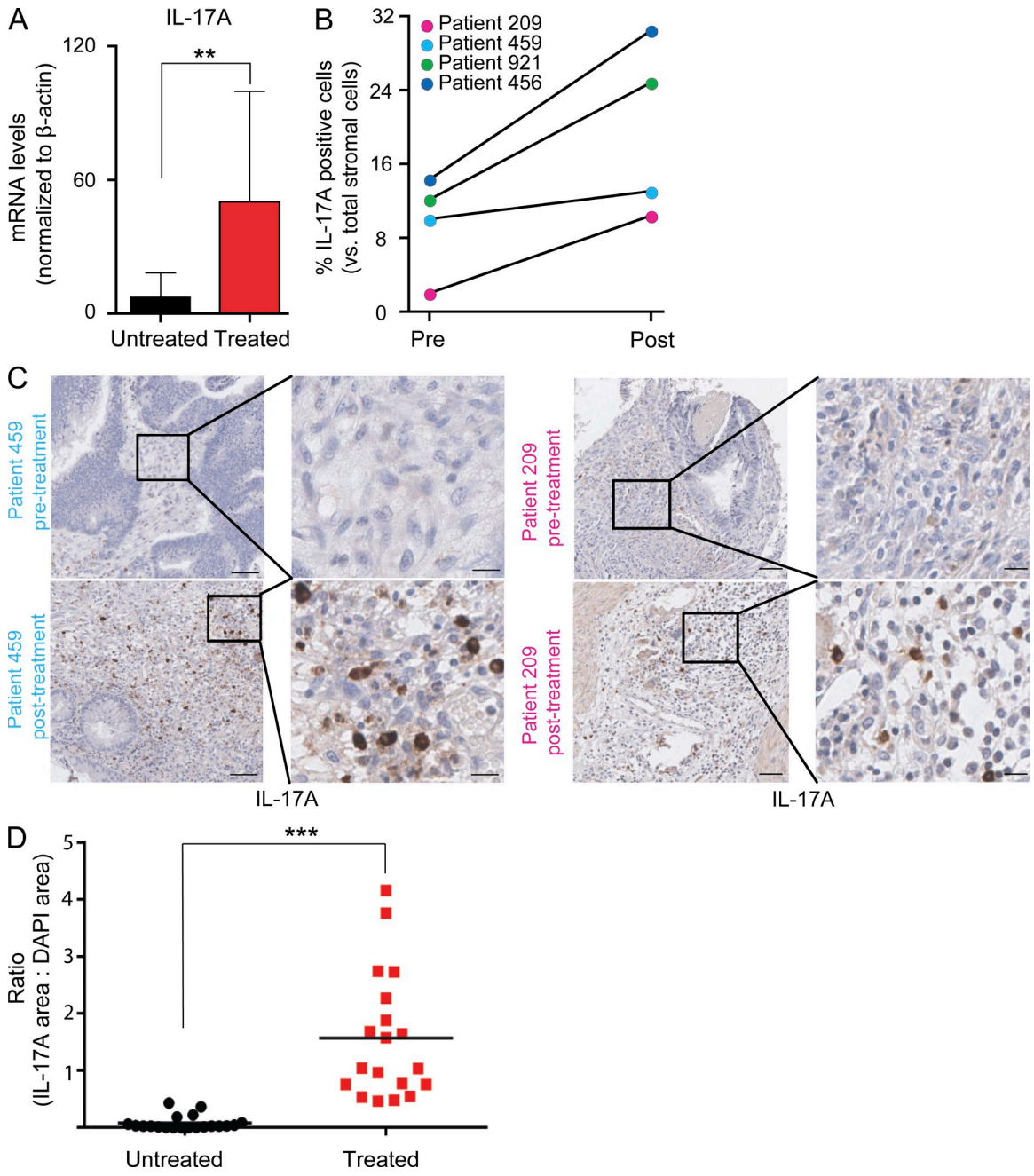

Figure 6. Cytotoxic treatment induces IL-17A in human specimens. (A) mRNA levels of IL-17A from untreated or treated patients (17 samples each group) were quantified by quantitative RT-PCR. Data are mean ± SD ($n = 20$); **, $P < 0.01$. Student's t test was used to assess the significance. The experiment was performed three times and representative data are shown. (B and C) Paraffin-embedded sections of matched human colorectal tumors before and after cytotoxic treatment from four patients were stained for IL-17A. The percentage of the IL-17A–positive cells was quantified as a percentage of the total stromal cells (B); $P < 0.05$. Student's t test was used to assess the significance. Two representative samples are shown (C). Bars: (C) 100 µm; (C, inset) 25 µm. (D) Protein levels of IL-17A from unmatched chemotherapy treated and untreated colorectal cancer specimens (20 patients in each group) were quantified using immunofluorescence staining. Frozen sections of human colorectal tumors were stained for IL-17A. Nuclei were counterstained with DAPI. Quantification was done by scanning three high-power fields per specimen using ImageJ software. Data are mean ratio of IL-17A area to DAPI area per patient. ***, $P < 0.001$. Student's t test was used to assess the significance.

in Tables S2 and S3). We also studied IL-17A protein expression before and after therapy in an additional four matched human tumors by immunohistochemistry (Fig. 6, B and C; and data not depicted). In each case evaluated, there was an increase in stromal expression of IL-17A protein, which was additionally confirmed in a cohort of 40 tumor specimens

Published December 9, 2013

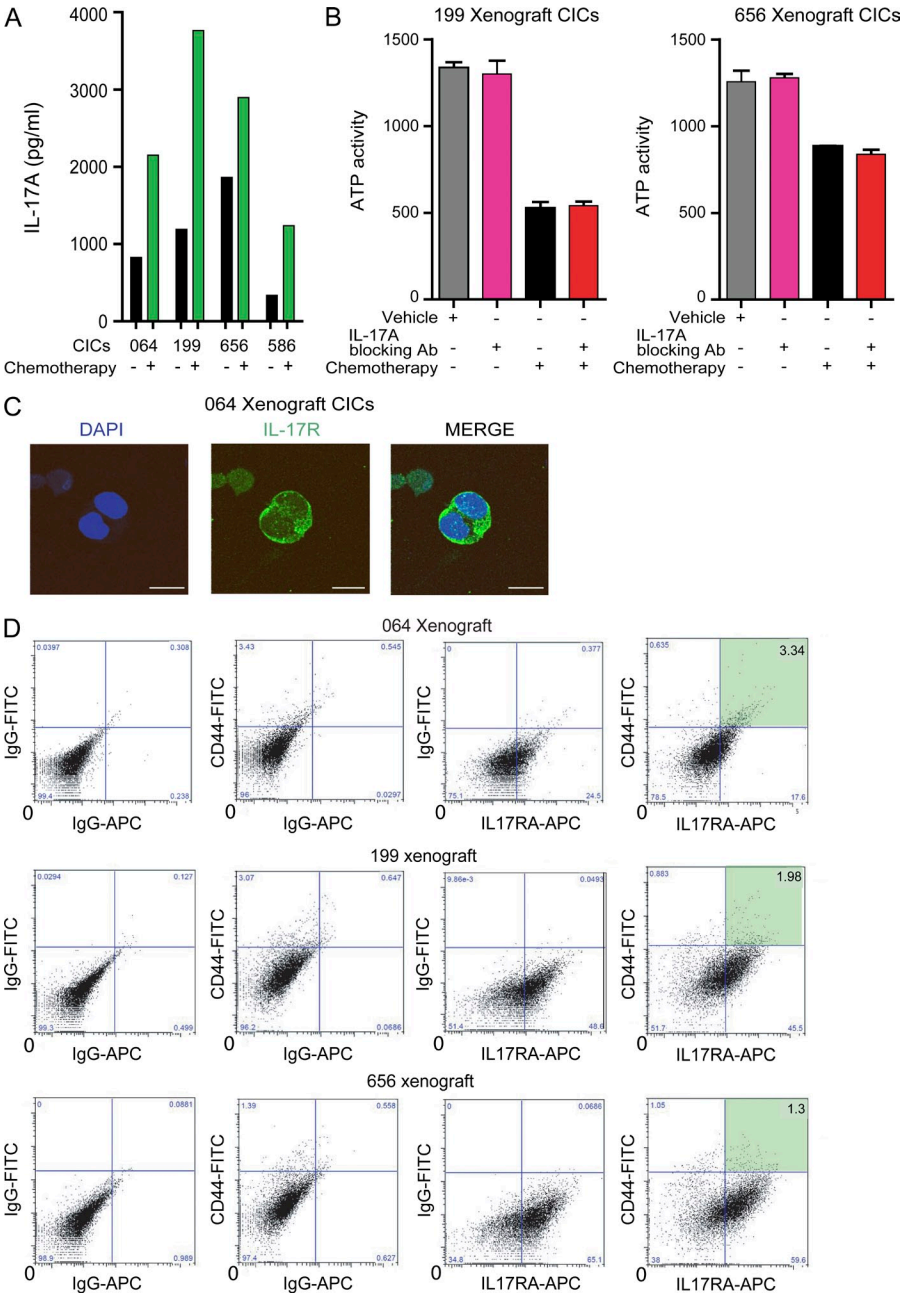

Figure 7. IL-17A can contribute to CICs maintenance through IL-17A receptor. (A) Autocrine expression of IL-17A was assessed using a 120 human cytokine antibody array from RayBio on 4 CICs treated with vehicle (DMSO) or with chemotherapy for 3 d. The mean concentration of IL-17A was statistically significant in the four CICs treated with chemotherapy compared to vehicle. ($n = 1$); $P < 0.01$. Student's *t* test was used to assess the significance. The experiment was performed once. (B) The autocrine IL-17A production was examined by studying the effects of IL-17A blockade on the tumor-initiating capacity of CICs in the absence of CAFs. The effects were assessed in two different specimens by 10 d of co-culture. 10^4 CICs were treated with vehicle (DMSO), chemotherapy alone, or along with IL-17A blocking antibody (15 ng/ml). Number of viable cells was measured by Cell Titer-Glo assay. No statistically significant difference in viability was noted as a result of IL-17A blocking antibody. Data are presented as mean ± SD ($n = 3$); unlabeled, $P > 0.05$. Student's *t* test was used to assess the significance. The experiment was performed twice, and representative data are shown. (C) IL-17RA was expressed in CICs as demonstrated by immunofluorescence staining. Nuclei were counterstained with DAPI. Bar, 10 µm. (D) Confirmation of IL-17RA expression was assessed in CICs by FACS analysis of single cells from three freshly dissociated xenografts co-stained for FITC-CD44 and APC-IL17RA.

from either untreated or treated patients (20 patients in each group; Fig. 6 D). Collectively, these results strongly suggest that CAFs respond to chemotherapy by the expression of defined factors including IL-17A that could instruct the cellular hierarchy.

IL-17A can contribute to CICs maintenance through IL-17A receptor

The vast majority of colorectal cancers are spontaneous but a subset of colorectal cancers occurs within the context of inflammatory bowel disease, particularly ulcerative colitis. This minority has been extensively modeled using genetically engineered mouse models of colitis to induce colorectal cancer. In these models, IL-17A is secreted by T-helper IL-17 (Th17) cells to regulate other immune elements and promote tumorigenesis (Wu et al., 2009). Our studies focus on models that represent spontaneous colorectal tumors in which inflammation is important but may be less central to disease pathology and, thus, other stromal elements may serve greater roles. We found that chemotherapy-treated CAFs directly augmented CIC growth in the absence of inflammatory cells, suggesting that IL-17A might directly regulate CICs. As prior studies have not determined involvement of IL-17A in CICs, we next sought to evaluate the direct contribution of IL-17A signals to CIC maintenance. First we analyzed IL-17A expression in CICs treated with vehicle or chemotherapy in

Published December 9, 2013

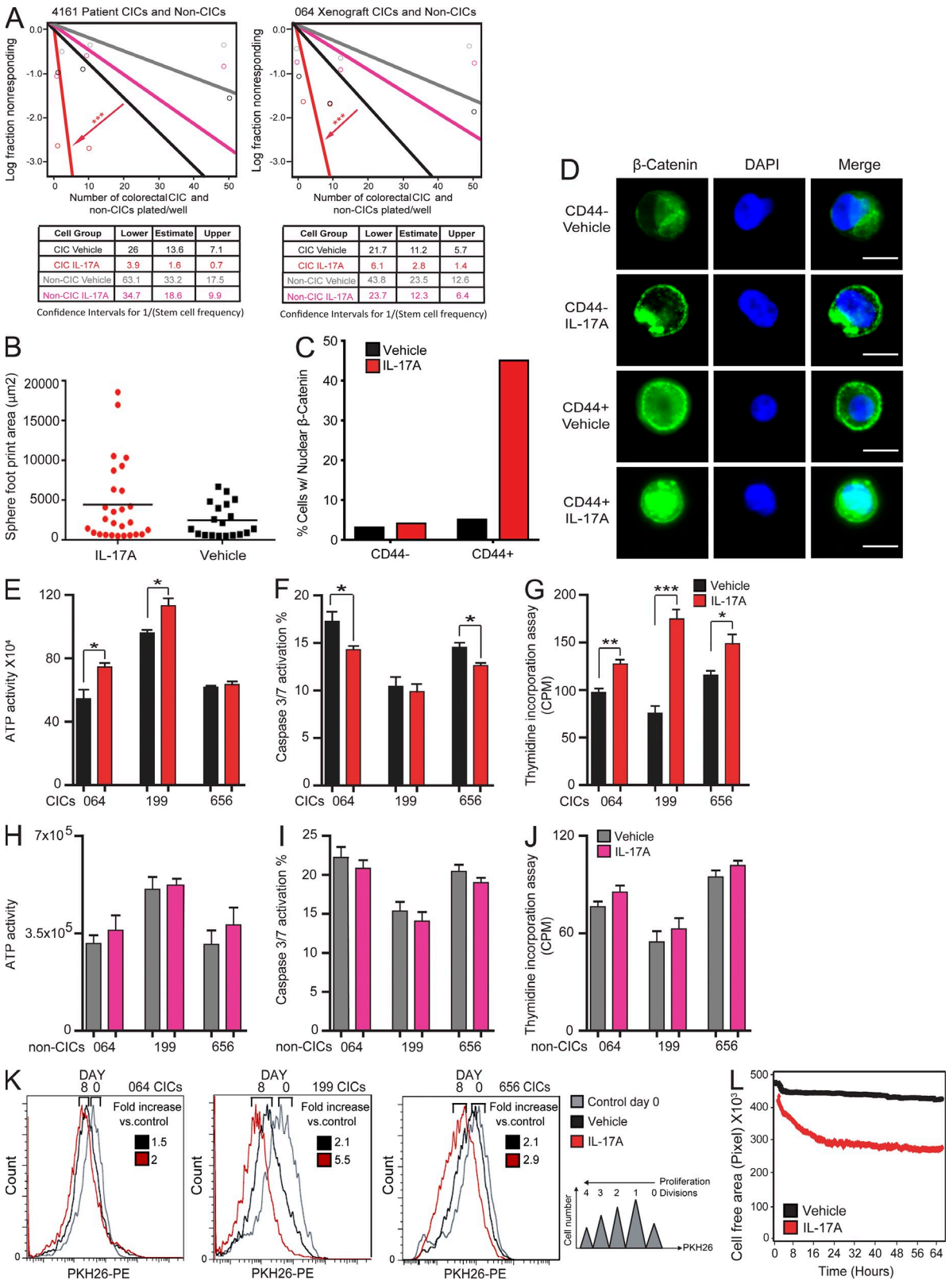

Figure 8. Exogenous IL-17A promotes colorectal sphere maintenance, proliferation, and migration. (A) CICs and non-CICs from two independent patient specimens were plated in limiting dilution (50, 10, or 1 cell[s] per well) in 96-well plates and tested for the effect of exogenous IL-17A (100 ng/ml). The presence of spheres was evaluated after 14 d. Data are mean ± SD (n = 20); ***, $P < 0.05$. Student's t test was used to assess the significance. The experiment was performed three times and representative data are shown. (B) The tumorspheres area from one specimen (064; sphere frequency/sphere

Published December 9, 2013

four different patients by cytokine array analysis and we showed the presence of moderate autocrine production of IL-17A that could contribute to their own hierarchy (Fig. 7 A). To clarify the potential role for autocrine effects of IL-17A, we examined the effects of IL-17A blockade on CIC's viability in the absence of CAFs using a neutralizing antibody (Fig. 7 B). In these studies, autocrine IL-17A appeared to function as a minor component in CIC maintenance relative to stromal IL-17A. These data suggest that the dominant role of IL-17A is a paracrine signal.

As the biological effects of IL-17A require target cell expression of the cognate receptor, we assessed IL-17A receptor (IL-17RA) expression in isolated CICs cultured short term as tumorspheres. The majority of CICs expressed IL-17RA, as measured by immunofluorescent staining and FACS analysis, whereas non-CICs less commonly expressed IL-17RA (Fig. 7, C and D), supporting a possible functional paracrine loop of CAF-derived IL-17A to IL-17RA on CICs.

IL-17A promotes protumorigenic CIC behavior

To interrogate the functional significance of IL-17A on CICs and non-CICs, we added exogenous IL-17A ligand to mimic the effects of IL-17A produced by CAFs. IL-17A enhanced CIC tumorsphere formation measured by in vitro limiting dilution (Fig. 8 A), with more modest effects on non-CICs. In addition, IL-17A modestly increased the size of the spheres formed compared with the untreated group (Fig. 8 B). Nuclear localization of β-catenin has been reported as a potential functional marker of CICs (Vermeulen et al., 2008). We therefore examined the effects of IL-17A signaling on the percentage of cells expressing nuclear β-catenin. IL-17A induced nuclear β-catenin localization in $CD44^{high/+}$ cells but not $CD44^{low/-}$ cells, confirming in limiting dilution studies (Fig. 8, C and D). IL-17A promoted increased CIC viability in ATP-dependent assays, cell survival, and DNA synthesis (Fig. 8, E–G). These effects were not detected in non-CICs (Fig. 8, H–J). Another phenotype associated with CICs, label retention, was increased in response to IL-17A treatment (Fig. 8 K). As CICs may contribute to tumor invasion and metastasis, we also demonstrated that exogenous IL-17A nearly doubled the CIC migration rate as measured by a scratch assay (Fig. 8 L).

To further evaluate the effects of IL-17A signal transduction on CICs, we generated genetically modified cells with IL-17A overexpression to mimic the effects of CAFs or IL-17RA knockdown to block the reception of IL-17A signals. We validated our viral transduction protocol using a GFP-containing vector. Efficacy of viral transduction was measured by FACS. 91.5% of transfected CICs were positive for GFP (unpublished data). IL-17A cDNA or IL-17RA shRNA resulted in an ∼80% up-regulation or reduction of IL-17A or IL-17RA mRNA, respectively (Fig. 9, A and B). When these genetically modified CICs were studied in an in vitro limiting dilution assay, IL-17A overexpression significantly increased tumorsphere formation, whereas IL-17RA knockdown decreased sphere formation (Fig. 9 C). Exogenous IL-17A also stimulated tumorsphere formation but this effect was more modest than ligand overexpression (Fig. 9 C), likely because of the sustained effects of secreted ligand. These data suggest that IL-17A broadly augments protumorigenic CIC behaviors.

To address the contribution of IL-17A in the in vivo growth of CICs using a clinically relevant method, we used an IL-17A neutralizing antibody in combination with chemotherapy (5-FU and Oxaliplatin). Tumors were established by injecting CICs in combination with CAFs subcutaneously in immunocompromised mice. The addition of the IL-17A neutralizing antibody augmented the efficacy of chemotherapy on tumor growth (Fig. 9, D and E), confirming CIC growth dependence upon chemotherapy treatment on IL-17A. These results provide a direct relevance for IL-17A targeting, even in the absence of a functional immune system.

IL-17A contributes to CIC therapeutic resistance

In concordance with IL-17A as an important regulator of the CIC phenotype, we found that IL-17A promoted basal CIC growth and protected CICs from chemotherapy-induced growth inhibition (Fig. 10 A). A neutralizing IL-17A antibody blocked the effects of chemotherapy treated CAFs on CIC growth in comparison to an IgG control (Fig. 10 B), confirming the importance of IL-17A for CAF effects on CICs. To define potential mechanisms through which IL-17A regulates CIC biology, we interrogated gene expression profiles of CICs isolated from three different patients treated

footprint using ImageJ software) was evaluated after 14 d. The mean area of spheres treated with IL-17A was 4,438.5 ± 960 μm² compared to 2,458.6 ± 481 μm² in the untreated group. P = 0.073. Student's *t* test was used to assess the significance. The experiment was performed once. (C and D) Cells were sorted for $CD44^{high/+}$ and $CD44^{low/-}$ and treated with IL-17A (100 ng/μl) for 12 h. (D) Cells were stained for β-catenin with DAPI nuclear background. Bar, 25 μm. (C) Beta-catenin localization was quantified. The experiment was performed once. (E–G) CICs cell viability, apoptosis, and proliferation of three independent specimens were assessed by (E) CellTiter-Glo, (F) caspase 3/7 activation, and (G) thymidine incorporation after stimulation with vehicle and exogenous IL-17A (100 ng/ml). Non-CICs from three independent specimens were plated and tested for the effect of exogenous IL-17A (H–J). Cell viability, apoptosis, and proliferation were assessed by CellTiter-Glo (H), caspase 3/7 activation (I), and thymidine incorporation (J) after stimulation with vehicle and exogenous IL-17A (100 ng/ml). Data are mean ± SD (n = 3); *, P < 0.05; **, P < 0.01; ***, P < 0.001; unlabeled, P > 0.05. Student's *t* test was used to assess the significance. The experiment was performed three times and representative data are shown. (K) Label retention of CICs from three independent patient specimens was evaluated by the staining with PKH-26-PE dye and the FACS analysis at day 0 (control) and after 8 d of stimulation with the vehicle and IL-17A. The experiment was performed once. (L) Migration of CICs from a human sample stimulated with exogenous IL-17A or a vehicle was evaluated by the scratch assay. The area of the scratch was monitored by time-lapse microscopy for 64 h. The experiment was performed twice and representative data are shown.

Published December 9, 2013

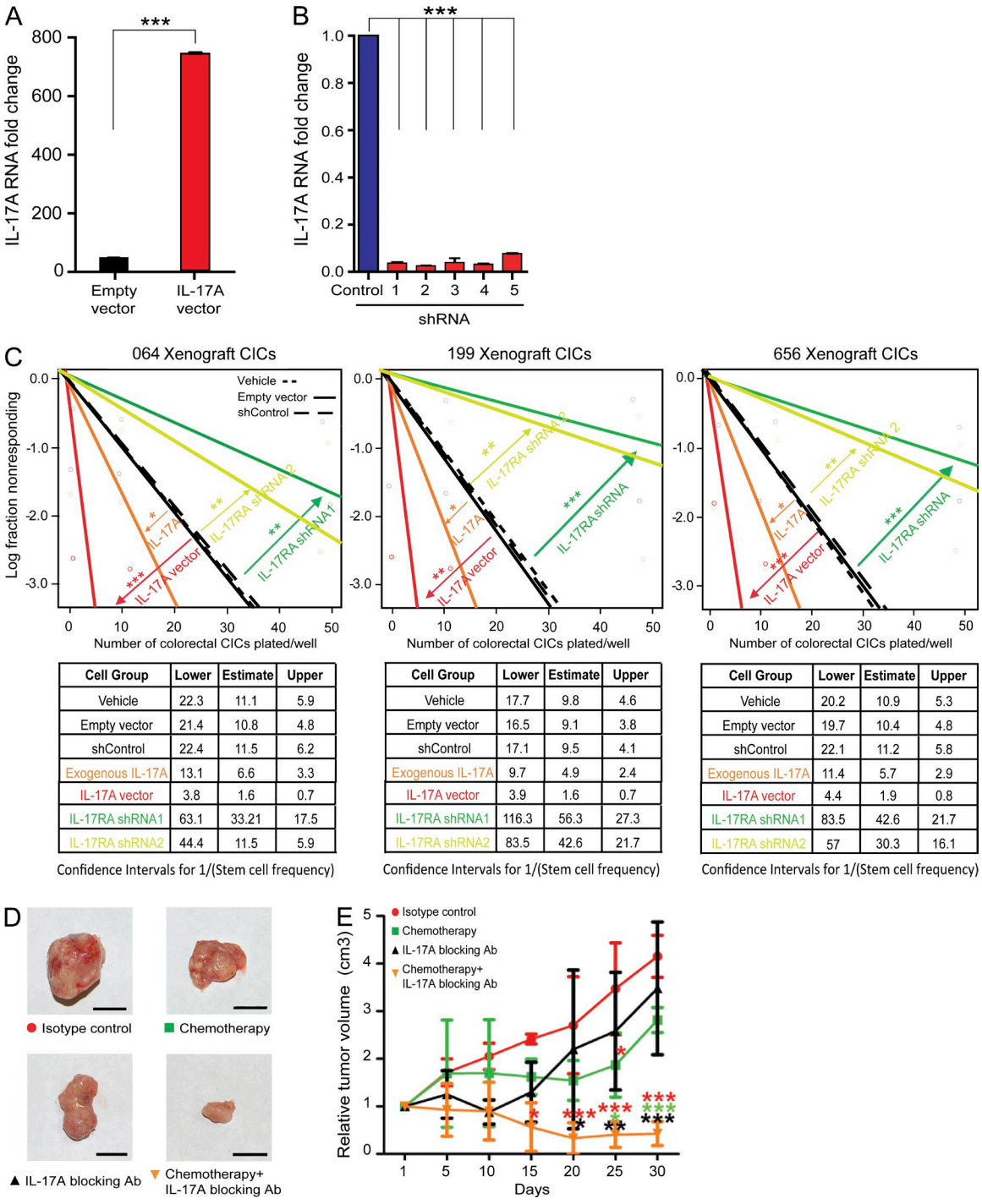

Cell Group	Lower	Estimate	Upper
Vehicle	22.3	11.1	5.9
Empty vector	21.4	10.8	4.8
shControl	22.4	11.5	6.2
Exogenous IL-17A	13.1	6.6	3.3
IL-17A vector	3.8	1.6	0.7
IL-17RA shRNA1	63.1	33.21	17.5
IL-17RA shRNA2	44.4	11.5	5.9

Confidence Intervals for 1/(Stem cell frequency)

Cell Group	Lower	Estimate	Upper
Vehicle	17.7	9.8	4.6
Empty vector	16.5	9.1	3.8
shControl	17.1	9.5	4.1
Exogenous IL-17A	9.7	4.9	2.4
IL-17A vector	3.9	1.6	0.7
IL-17RA shRNA1	116.3	56.3	27.3
IL-17RA shRNA2	83.5	42.6	21.7

Confidence Intervals for 1/(Stem cell frequency)

Cell Group	Lower	Estimate	Upper
Vehicle	20.2	10.9	5.3
Empty vector	19.7	10.4	4.8
shControl	22.1	11.2	5.8
Exogenous IL-17A	11.4	5.7	2.9
IL-17A vector	4.4	1.9	0.8
IL-17RA shRNA1	83.5	42.6	21.7
IL-17RA shRNA2	57	30.3	16.1

Confidence Intervals for 1/(Stem cell frequency)

Figure 9. IL-17A/IL-17RA signaling regulates colorectal CIC growth and self-renewal. (A) Quantitative RT-PCR analysis of IL-17A in CICs overexpressing IL-17A. Data are mean ± SD ($n = 3$); ***, $P < 0.001$. Student's t test was used to assess the significance. The experiment was performed three times and representative data are shown. (B) Quantitative RT-PCR analysis of five different shRNAs for IL-17RA in CICs. Data are presented as means ± SD ($n = 3$); ***, $P < 0.001$. Student's t test was used to assess the significance. The experiment was performed three times and representative data are shown. (C) Effects of IL-17RA knockdown with two different shRNAs (shIL-17RA1 or shIL-17RA2) or IL-17A overexpression with IL-17A transduction on tumorsphere formation. 064 and 199 and 656 CICs transduced with two different shRNAs or shControl and with IL-17A vector or empty vector were plated in replicates in stem cell media in a limiting dilution assay, and were then analyzed for the presence of spheres after 14 d. Data are mean ± SD ($n = 20$); *, $P < 0.05$; **, $P < 0.01$; ***, $P < 0.001$. The likelihood ratio test was used to assess the significance. The experiment was performed two times and representative data are shown. (D, E) The dependence of CICs on IL-17A was evaluated in vivo. 104 CICs and 3×10^4 CAFs were injected into mice. When tumors were established to approximately 0.3 cm^3 in volume, treatment was initiated. Four arms were included: isotype control (2 mg/kg antibody five times a

Published December 9, 2013

with and without IL-17A. Heat maps illustrate the common effects of IL-17A (Fig. 10 C) on the repression and activation of subsets of genes within CICs. When these genes were analyzed to determine the pathways altered by IL-17A treatment, NF-κB signaling was found to be highly elevated (IPA Ingenuity Systems; Fig. 10 D). We confirmed activation of the NF-κB pathway and its downstream target ERK1/2 at the protein level through the analysis of the levels of the phosphorylation status of NFκBp65 (RelA) and p42-44-ERK1/2 in CICs treated with vehicle or with IL-17A for 12 h (representative immunoblot, Fig. 10 E). The specificity of this effect was confirmed by the addition of an IL-17A–blocking antibody to restore the basal phosphorylation level confirming the direct connection between IL-17A and the NF-κB activation (Fig. 10, D and E). These data suggest that IL-17A up-regulation of NF-κB is a possible contributing mechanism through which CIC maintenance is promoted and that targeting of NF-κB or its target genes may inhibit the effects of CAF produced IL-17A after cytotoxic treatment. As NF-κB has been associated with CIC maintenance (Schwitalla et al., 2013), our results add an additional layer of microenvironmental signals that may enforce tumor growth.

DISCUSSION

Stem cells are essential contributors to maintenance of tissue homeostasis and recovery from injury. However, the sustained proliferative potential of stem cells must be tightly constrained to prevent cancer. The functional location or niche in which a stem cell resides provides maintenance cues and restrains uncontrolled growth. When a stem cell exits its niche, it undergoes lineage specification and differentiation, providing an essential role for the microenvironment in normal cellular hierarchies (Schuijers and Clevers, 2012). As cancers mimic development and wound responses (i.e., "the wound that does not heal"; Dvorak, 1986; Schäfer and Werner, 2008), two scenarios in which stem cells function, it is not surprising that cancers display cellular hierarchies and coopt stem cell regulatory mechanisms. This has been shown first in leukemia (Bonnet and Dick, 1997) and, more recently, in several solid cancers, including colorectal cancers (Dalerba et al., 2007). Single hematopoietic stem cells repopulate the entire systemic blood system, and these cells rapidly home to the bone marrow niche for instructive cues to sustain this process. Organ regeneration by single stem cells is less evident in solid tissues, and recent work in the colon has shown that intestinal epithelial stem cells display a synergistic relationship with supportive $CD24^+$ (or $cKit^+$) accessory cells, similar to Paneth cells in the small intestine (Sato et al., 2011). Stem cell–Paneth cell doublets potently proliferate relative to single stem cells (Sato et al., 2011). This relationship demonstrates a functional complementation between specialized client cells and accessory cells that provides signals to promote client cell adaptation and defend the homeostatic state under noxious conditions. This hypothesis has been advanced by Medzhitov and Horng (2009) within the context of macrophage function in inflammatory responses. Based on this background, our results suggest that colorectal cancers respond to noxious conditions (cytotoxic treatment) by stimulating accessory cells (CAF) to provide signals (IL-17A) to support a homeostatic state (maintenance of the cellular hierarchy). Disruption of this circuit through targeted therapies may sensitize the chemotherapy-resistance commonly found in colorectal cancers.

Although several studies have examined the cellular hierarchy within colorectal cancers, many have used cell lines that have been forced to acquire self-renewal mechanisms in the absence of the tumor microenvironment. Our studies were devoted to dissecting a single cell–cell interaction in a more complex system. An elegant genetically engineered mouse model of colon cancer described a role of a long term passaged, immortalized normal colon fibroblast cell line in the self-renewal of early transformed colon cells associated with expression of HGF (Vermeulen et al., 2010). As most lethal colorectal cancers are diagnosed at more advanced stages, we used a clinical relevant strategy based on human CAFs (rather than a modified normal fibroblast) and colorectal cancer cells directly derived from patients. Using these resources, we recognized increased CAF frequency in patient tumors after cytotoxic treatment, suggesting that CAFs may function in regenerating the aberrant organ system in colorectal cancers. Chemotherapy-stimulated CAFs produced a secretome that enhanced CIC proliferation and tumorigenesis. As cytokines offer important instructive cues from supportive accessory cells, we focused our attention on these molecules within the secretome. We found that chemotherapy potently induced IL-17A in CAFs that directly augmented the growth of CICs. Of note, we also found that chemotherapy induces expression of CAF TGFβ, a chemokine with a well-established role in the cancer microenvironment. Alterations in TGFβ pathway components affect 40–50% of all colorectal cancers (Markowitz et al., 1995; Markowitz and Bertagnolli, 2009). In the tumor microenvironment, TGFβ induces transdifferentiation of normal fibroblasts to CAFs, i.e., morphological changes and up-regulation of α-SMA. (Lieubeau et al., 1994; Tuxhorn et al., 2002). In addition, TGFβ activates colorectal cancer CAFs to secrete various cytokines that exert a prosurvival signal on cancer cells (Calon et al., 2012) and stromal TGFβ signaling is required for the

week for two weeks and then once a week for two weeks), chemotherapy alone (Oxaliplatin: 0.25 mg/kg once a week for 4 wk; 5-FU: 15 mg/kg five times a week for 2 wk), IL-17A blocking antibody alone (2 mg/kg five times a week for 2 wk and then once a week for 2 wk) or a combination of the IL-17 antibody and chemotherapy (four mice per arm). Mice were weighed and the tumor volume was measured every other day for 30 d. Mice were sacrificed and tumors were collected. (D) Representative images of treated tumors and (E) relative tumor volume. Bar, 1 cm. Data are presented as mean ± SD ($n = 4$); *, $P < 0.1$; **, $P < 0.05$; ***, $P < 0.001$. ANOVA, followed by Bonferroni's post-hoc test was used to assess the significance.

Published December 9, 2013

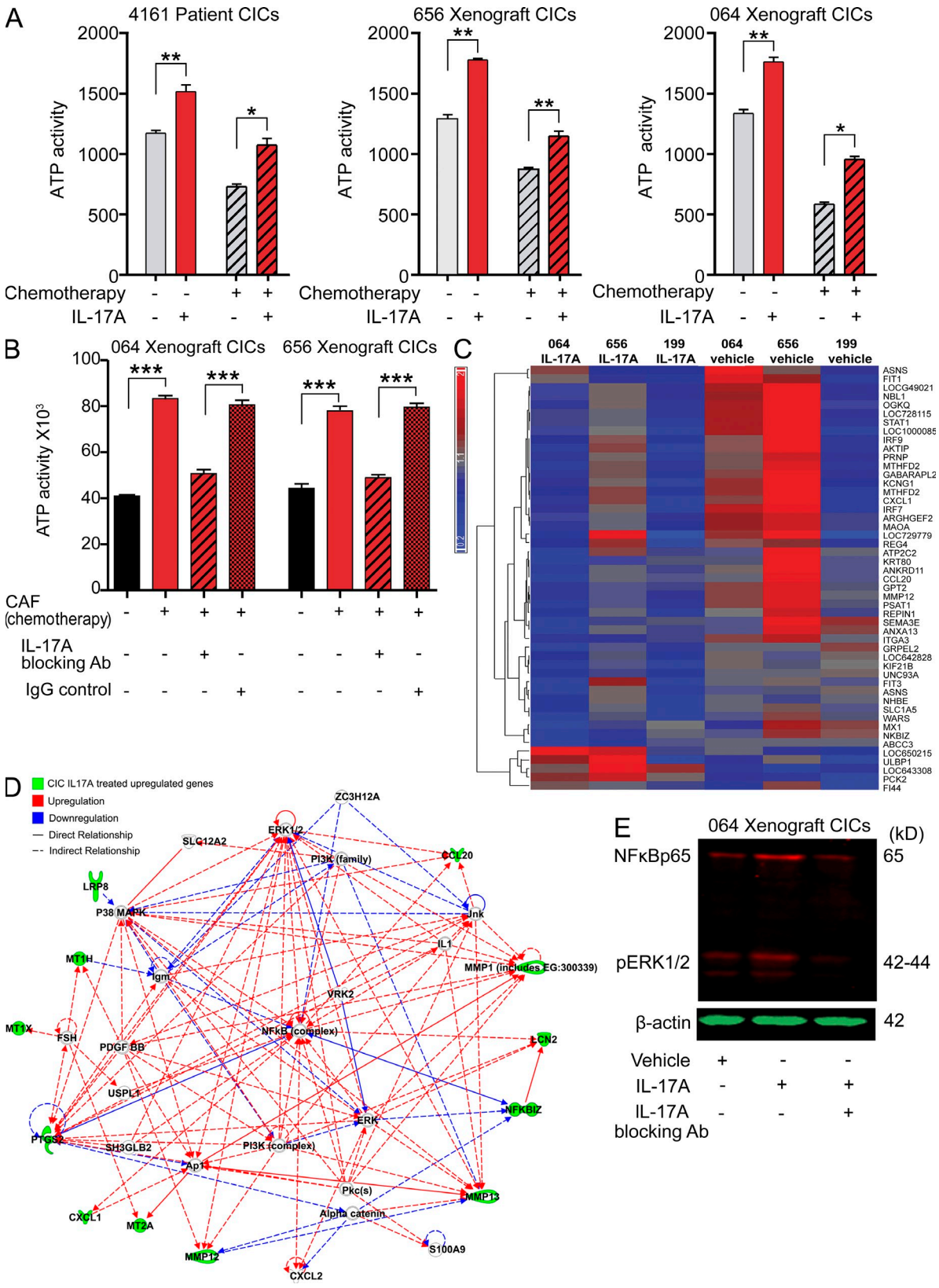

Figure 10. Exogenous IL-17A promotes chemoresistance through the NF-κB pathway. (A) Chemosensitivity of 3×10^3 CICs from the three independent human samples stimulated with exogenous IL-17A and treated with chemotherapy was evaluated by CellTiter-Glo assay. Data are mean ± SD ($n = 3$); *, $P < 0.05$; **, $P < 0.01$. Student's t test was used to assess the significance. The experiment was performed three times and representative data

Published December 9, 2013

initiation of colorectal cancer metastasis (Calon et al., 2012). Although TGFβ has been linked to CIC growth in glioblastoma (Peñuelas et al., 2009), we did not find that TGFβ directly enhanced colorectal CIC growth (unpublished data). However, our results support potential interactions of multiple cellular components within tumors as TGFβ induces IL-17A in $CD8^+$ splenocytes in tumor-bearing mice (Schäfer and Werner, 2008), suggesting that chemotherapy treatment may stimulate IL-17A expression both directly by CAFs and indirectly through TGFβ effects on the immune system. This model would explain why targeting IL-17A largely inhibited the direct effects of CAFs on CICs, thus augmenting the importance of this pathway in colorectal cancer.

Prior delineation of the role of IL-17A in colorectal cancer has come from either models of colitis-associated cancers (Hyun et al., 2012), induction of tumor formation from colonic bacteria (Wu et al., 2009; Grivennikov et al., 2012), and promoting tumor resistance to antiangiogenic therapy (Chung et al., 2013). These studies have largely focused on the interplay between IL-17A and the immune system, including Th17 cells. As we were able to isolate the paracrine relationship between CAFs and tumor cells, future studies will combine these observations with interactions between the immune system and both CAFs and tumor cells.

IL-17A has been the subject of intense research not only in basic laboratory studies, but has already translated into the development of pharmacologic inhibitors, primarily for autoimmune conditions. Although targeting IL-17A has been effective in treating psoriasis (Leonardi et al., 2012; Papp et al., 2012), anti–IL-17A agents have proven less effective against Crohn's disease, suggesting that combination strategies may be required for some diseases in which IL-17A is functionally important (Hueber et al., 2010). Our studies suggest that IL-17A may also function indirectly in chemotherapy resistance through remodeling of the tumor microenvironment, suggesting a potentially more nuanced role and application within therapeutic paradigms. Indeed, we are currently developing preclinical targeting strategies to compare both genetic and pharmacologic inhibition in chemotherapy-induced tumor remodeling. These results suggest that chemotherapy may also serve as a "double-edged sword" due to effects on enriching CICs that are relatively less chemosensitive and altering the tumor microenvironment through effects on CAFs. We are actively investigating these elements as well as the interactions between tumor genotype and these tissue stress responses. To date, we have found no differences in the responses of CAFs to chemotherapy in IL-17A production or response of CICs to IL-17A treatment based on their genetics (e.g., *KRAS* mutations, microsatellite stable versus unstable). Collectively, these results and those of other groups studying a role of IL-17A in the early induction of colorectal tumorigenesis strongly suggest that cytokines produced in response to cytotoxic treatment may function to support the development and maintenance of colorectal cancers and offer novel therapeutic targeting strategies.

MATERIALS AND METHODS

Isolation and culture of CICs and CAFs. All human tissues were acquired from primary human colorectal tumor patient specimens according to human experimental guidelines. Human protocols were approved by the Institutional Review Board of the Cleveland Clinic Foundation (protocol number: IRB 4134). Tumor specimens were maintained through subcutaneous xenografts in the flanks of NOD-SCID/IL2Rγnull (NSG) mice. Tumors were dissociated using a papain dissociation system (Worthington Biochemical). $CD44^{high/+}$ cells (enriched in CICs) were enriched by flow cytometry (FACS Aria II) and grown as tumorspheres at 37°C in an atmosphere of 5% CO_2. CICs were cultured in serum-free media with basic fibroblast growth factor (bFGF, 10 ng/ml; R&D Systems) and epidermal growth factor (EGF, 10 ng/ml; R&D Systems). For isolation of CAFs, surgical specimens were similarly dissociated into single-cell suspension, and PDGFRα-expressing cells were sorted using flow cytometry (FACS Aria II). Cells were then cultured in DMEM with 10% BSA. For cell counting before each experiment, a single-cell suspension was achieved using TrypLE (Invitrogen) dissociation.

Flow cytometric analysis. Flow cytometry was performed using a FACSAria II Cell Sorter (BD). To enrich for CICs. Single cells were labeled with a phycoerythrin-conjugated monoclonal antibody against CD44 (Miltenyi Biotec), and then analyzed for the expression of phycoerythrin-conjugated monoclonal antibody against CD133 (Miltenyi Biotec), FITC monoclonal antibody against EpCAM (R&D Systems), and ALDH with ALDEFLUOR assay (ALDAGEN). To enrich for PDGFRα-positive CAFs, single cells were labeled with phycoerythrin-conjugated monoclonal antibody against PDGFRα (R&D System). To analyze the expression of IL-17RA within the CIC population, single cells were double labeled with FITC-CD44 (Miltenyi Biotec) and APC-IL17RA (R&D Systems). Dead cells were eliminated by using the viability dye DAPI. Side scatter and forward scatter profiles were used to eliminate cell doublets. Isotype controls were used to establish proper gates. The "high positive" population was gated in a range of 4–10% (depending on the percentage of the total positive cell population of each sample) of the tail of the positive cells.

Immunoblotting. CICs from 3 different patients were treated with vehicle, 100 ng/ml IL-17A ± 15 ng/ml IL-17A blocking antibody (R&D Systems). Lysates were harvested 12 h after treatment and immunoblotted. The membrane was simultaneously probed for anti–NF-κB p65 (Cell Signaling

are shown. (B) The effect of the media conditioned by CAFs on CICs from two different specimens was assessed by ten-day co-culture. 10^4 CICs were cultured with 2×10^4 CAFs treated with vehicle (DMSO), chemotherapy alone or along with IL-17A blocking antibody (15 ng/ml), or an isotype IgG control. Cell growth was measured by CellTiter-Glo assay. Data are mean ± SD ($n = 3$); **, $P < 0.01$; ***, $P < 0.001$. Student's t-test was used to assess the significance. The experiment was performed three times and representative data are shown. (C) CICs gene profile from three independent human samples stimulated with vehicle or exogenous IL-17A was performed on an Illumina expression array. Signal data were filtered to include only genes that were seen to have changes in at least two of the three matched pairs and were subjected to hierarchical clustering. Signal ratio > 1.5 and $P < 0.05$. (D) Network analysis of the most significant genes up-regulated in CICs stimulated with IL-17A versus vehicle was generated using IPA (Ingenuity Systems). (E) The alteration of the NF-κB pathway and its downstream target ERK1/2 was assessed at the protein level through the analysis of the levels of the phosphorylation status of NF-κB p65 (RelA) and p42-44-ERK1/2 in one sample treated with vehicle or with IL-17A with and without the IL-17A blocking antibody for 12 h.

Published December 9, 2013

Technology), p42/44ERK1/2 (Cell Signaling Technology), and anti–β-actin (Sigma-Aldrich). Secondary detection was accomplished using IRDye 800 and IRDye 680 detected on the Odyssey imaging system (Li-Cor).

Quantitative RT-PCR. Total cellular RNA was isolated with the RNeasy kit (QIAGEN) and reverse-transcribed into cDNA using the SuperScript III Reverse Transcription kit (Invitrogen). Real-time PCR was performed on an Applied Biosystems 7900HT cycler using SYBR Green Master mix (SA Biosciences) and gene-specific primers, as follows: β-actin forward (5′-AGAAAATCTGGCACCACACC-3′) and reverse (5′-AGAGGCGTACAGGGATAGCA-3′), CD44 forward (5′-GCCCTTCCATAGCCTAATCC-3′) and reverse (5′-CTTTGGTGTCTCCCAGAAGC-3′), Sox-9 forward (5′-CCTGCCCTTCTGGTTCCG-3′) and reverse (5′-TCCTCGTCCCTCTCTTTCTTCAG-3′), ALDH1 forward (5′-TGGCTTATCAGCAGGAGTGT-3′) and reverse (5′-GCAATTCACCCACACTGTTC-3′), IL-17A forward (5′-AAGACCTCATTGGTGTCACTGCTAC-3′) and reverse (5′-ATCTCTCAGGGTCCTCATTGCG-3′), IL-17RA forward (5′-AGACACTCCAGAACCAATTCC-3′) and reverse (5′-TCTTAG AGTTGCTCTCCACCA-3′), OCT4 forward (5′-TCTCCCATGCATTCAAACTGAG-3′) and reverse (5′-CCTTTGTGTTCCCAATTCCTTC-3′), BMI1 forward (5′-CCAGGGCTTTTCAAAAATGA-3′) and reverse (5′-GCATCACAGTCATTGCTGCT-3′), c-MYC forward (5′-TCAAGAGGCGAACACACAAC-3′) and reverse (5′-GGCCTTTTCATTGTTTTCCA-3′), MSI1 forward (5′-CCAATGGGTACCACTGAAGC-3′) and reverse (5′-ACTCGTGGTCCTCAGTCAGTCAGC-3′), DTK forward (5′-TGCTGGCAGAGGACATGA-3′) and reverse (5′-ACAGACAGCTGGCCCAAG-3′) TGFβ forward (5′-GCCTTTCCTGCTTCTCATGG-3′) and reverse (5′-TCCTTGCGGAAGTCAATGTAC-3′).

In vitro limiting dilution assay. CICs were flow sorted into 96-well plates at a final cell number per well of 1, 10, 50. Tumorsphere formation was evaluated 7 and 14 d after sorting, and wells were scored positive or negative for the presence of at least one tumorsphere. The estimated stem cell frequency was calculated using extreme limiting dilution analysis (Hu and Smyth, 2009).

In vivo tumorigenic potential. All animal studies described were approved by the Cleveland Clinic Foundation Institutional Animal Care and Use Committee and conducted in accordance with the National Institutes of Health Guide for the Care and Use of Animals. For subcutaneous tumors studies, 3×10^3 CICs from a xenograft originally derived from a primary colorectal cancer patient specimen (064) were implanted alone and along with 10×10^3 fibroblasts treated for 3 d with vehicle or chemotherapy: 5-Flurouracil (50 μg/ml) + Oxaliplatin (10 μM) + Leucovorin (1 μM) into the flanks of 20 (5 mice per condition) 6-wk-old female NSG mice were obtained from The Jackson Laboratory. Tumors were monitored, and after 1 wk from the first tumor growth, all the mice were sacrificed and tumors were removed and weighed to evaluate the tumor development, and then dissociated (see following paragraph).

In vivo evaluation of the dependence of CICs on IL-17A. 10^4 CICs and 3×10^4 CAFs were implanted into mice. When established tumors reached ∼0.3 cm^3 in volume, treatment was initiated. Four arms were included: isotype control (2 mg/kg antibody 5 times a week for 2 wk and then once a week for 2 wk), FOLFOX chemotherapy alone (oxaliplatin:, 0.25 mg/kg once a week for 4 wk; 5-FU, 15 mg/kg 5 times a week for 2 wk), IL-17A blocking antibody alone (IL-17A blocking antibody, 2 mg/kg 5 times a week for 2 wk and then once a week for 2 wk), or a combination of the IL-17 antibody and FOLFOX chemotherapy (4 mice per arm). Mice were weighed and the tumor volume was measured every other day for 30 d. Mice were sacrificed and tumors were collected and analyzed.

Cell growth and survival assays. 3,500 freshly sorted CICs and non-CICs cancer cells per well were plated in triplicate into 96-well plates containing appropriate growth media. The next day, vehicle or chemotherapy was added to the plate. Readings of ATP levels for viability (CellTiter-Glo, Promega) or apoptosis (Caspase-Glo 3/7, Promega) were performed using a luminometer (Perkin-Elmer).

Immunofluorescent imaging. Tumorspheres dissociated at single cells were cytospin (Shandon Cytospin4, Thermo) in PBS with 0.5% BSA. Cells were then post-fixed/permeabilized in 4% PFA, blocked in 5% normal goat serum, 0.1% TritonX-100 in 1XPBS and immunostained for anti-IL-17RA (R&D System) overnight at 4°C. $CD44^{high/+}$ cells sorted from primary xenograft were treated for 12 h with vehicle or IL-17A and stained for β-catenin (Abcam). Cancer associated fibroblasts cultured on coverslips were stained for PDGFRα, VIMENTIN, αSMA, FAP, EpCAM, SMOOTHELIN, high molecular weight CALDESMON (Abcam) overnight at 4°C. Secondary detection was accomplished using highly cross-adsorbed secondary fluorescently labeled antibodies (Invitrogen) for 1 h at room temperature. Nuclei were counterstained with DAPI (Invitrogen). For immunostaining analyses of tissue sections, 10-μm frozen sections were fixed, permeabilized, and stained for Il-17A (RD Systems), KI67 (Abcam) as describe above. Images were taken on an upright microscope (microscope make and model: Leica DM4000B; magnification/aperture: 10× 0.3NA- 20× 0.5NA- 40× 0.75NA; room temperature; imaging medium: air (glass coverslipped slides); fluorochromes: 488 and 568; camera make and model: QImaging Exi aqua; acquisition software: Qcapture pro6).

Immunohistochemistry imaging. Paraffin-embedded sections of human colorectal tumors matched before and after treatment from four patients were stained for IL-17A. The percentage of the IL-17A–positive cells versus the total stromal cells was quantified.

Immunohistochemistry/immunofluorescence imaging quantification. Images of pre- and post-chemotherapy tissues cross sections were acquired using a DM6000 upright microscope (Leica), a 10× 0.3NA objective, and a Retiga 2000R CCD digital camera (Q-Imaging; room temperature, imaging medium: air (glass coverslipped slides), fluorochrome: 488 and 568). Image acquisition was fully automated for up to eight slides using an eight-slide, linearly encoded X, Y, Z-motorized stage (Prior Scientific) managed by Objective Imaging's Oasis 4i controller, TurboScan software (Objective Imaging), and Image-Pro Plus 7.0 (Media Cybernetics).

During acquisition, high-magnification (auto-focused) image fields were acquired across the entire tissue section and stitched together to form a single high-resolution, large field-of-view (FOV) image. Each image field was background corrected before stitching to ensure continuity and account for lens-induced vignetting. In brief, for each cross section, the stromal channel was loaded, spectrally filtered to cluster regions, and thresholded (by size and morphology) to generate a binary mask. A Euclidean distance transform was then applied to this mask and multiplied by the stromal "skeleton" (medial axis thinning of stromal regions) to determine pixel by pixel stromal thickness. Similarly, the epithelial channel was also loaded and morphologically processed to generate a binary mask. Stromal thickness values and epithelial/stromal segmented areas were subsequently exported to Excel and these segmented regions and thickness measurements (stromal mask based restricted dilation) were pseudocolored and superimposed upon the original images. Finally, for the calculation of intensity distribution, the stromal and epithelial masks were multiplied by their respective extracted channels and thresholded in bins of 10 gray values to calculate area of staining per intensity bin. These values were also exported to Excel for each channel.

CIC growth in co-culture assay. 2×10^4 CAFs pretreated with vehicle (DMSO) or chemotherapy (5-flurouracil (50 μg/ml) + oxaliplatin (10 μM) + leucovorin (1 μM)) for 3 d were plated in triplicate into the top part (with 3 μm pores) of a 24-well co-culture plate in serum-free media. 10^4 freshly sorted colorectal $CD44^{high/+}$ cancer cells were plated in triplicate into the bottom of the co-culture plates. IgG control and IL-17A–blocking antibodies (15 ng/ml; R&D Systems) were used as indicated. After 10 d, ATP levels (CellTiter-Glo; Promega) were performed using a luminometer (Perkin-Elmer). Data are mean ± SD ($n = 3$); **, $P < 0.01$; ***, $P < 0.001$.

Thymidine incorporation assay. 2×10^4 CICs were plated in triplicate in 12-well plates, incubated for 4 h at 37°C, and washed in cold PBS and then 10% TCA. After 1-h incubation at 4°C in 10% TCA, cells were resuspended in 0.2 N NaOH and incubated at room temperature overnight. Samples were then placed in scintillation tubes with 9 ml of scintillation fluid and vortexed to break up thymidine precipitates. The count per minute of the thymidine-positive cells was taken using LS6500 Scintillation Counter (Beckman Coulter).

Cytokine array. The cytokine secretion of CAFs or CICs treated with vehicle control (DMSO) or chemotherapy for 3 d was assessed using a 120 human cytokine antibody array from RayBio. This membrane-based cytokine is designed to simultaneously detect expression levels of multiple cytokines, including the one that are normally involved in disease processes like cancer. This array has been previously used by Vermeulen et al. (2008, 2010).

Gene array. The Illumina microarray study comprised three matched pairs of CICs samples. Each pair had a treated (100 ng/ml IL-17A for 7 d) and an untreated sample. The normalized gene signals, p-values, and annotations were imported into MS access a database manager and processed. For a matched pair of samples, the gene signal ratio was calculated. Records were then filtered using these criteria.

A record passed the filter and was deemed an increase in gene expression if the signal ratio of treated/untreated samples was greater than or equal to 1.5 and the p-value of the gene in the treated sample was ≤0.05 (i.e., detected as present). A record passed the filter and was deemed a decrease in gene expression if the signal ratio of treated/untreated samples was ≤0.6666666 and the p-value of the gene in the untreated sample was ≤0.05 (i.e., the gene transcript had to be detected as present in the untreated sample if we are to truly believe it has decreased in the treated sample).

Changes found within the three matched pairs were collated into a master table and sorted into groups of genes that had been observed to have changed in all three matched pairs, in two of three and in only one of the three. If all changes were included, the total number would be 821 genes. If we trimmed the data to include only genes that were seen to have changes in at least 2 of the 3 matched pairs, the list fell to 49.

Signal data were median-normalized to prepare for importation into the software Partek Genomics Suite ver6.4. Principal component analyses were conducted to get a sense of how the whole expression profiles behaved within each group.

Signals were filtered using the 821 gene filter list and the 49 gene filter list and the expression pattern, resulting in these respective filters were subjected to hierarchical clustering. Samples were fixed and genes profiles were clustered. A Pearson dissimilarity metric with complete linkage was used to segregate profiles into various hierarchical groups.

Signal data were filtered to include only genes that were seen to have changes in at least two of the three matched pairs and were subjected to hierarchical clustering. Signal ratio > 1.5 and p-value < 0.05.

PKH26 analysis. CICs were stained for 5 min with 1:250 PKH-26 dye (Sigma-Aldrich), blocked with 1% BSA, washed twice and FACS analyzed with a FACS LSR II (BD) equipped with a 488-nm laser and a band-pass 575/26 nm optical filter. CICs were then divided, plated, and stimulated with vehicle and IL-17A (100 ng/ml) and, after 1 wk, the analysis was repeated.

Migration assay and time-lapse imaging. CICs stimulated with vehicle or 100 ng/ml exogenous IL-17A were plated in 6-well plates and allowed to attach. Upon full confluence, the plate was scratched with a pipet tip and the ability of the cells to migrate in that area was monitored and imaged for 64 h on a Leica DMIRB Inverted Microscope equipped for time-lapse microscopy with a Leica DFC420 camera, temperature controller (37°C), CO_2 (5%) incubation chamber (Leica), PeCon incubator (PeCon GmbH), prior motorized stage with linearly encoded controller with $x/y/z$ drive for time-lapse imaging of multiples fields, Uniblitz shutter (Vincent Associates), and MetaMorph Software (Molecular Devices). Images of multiple fields per well were collected every 3 min for 72 h using a dry 10×, 0.3 NA objective lens, and phase-contrast optics.

Vectors and lentiviral transfection. Lentiviral clones expressing shRNAs specific to IL-17RA (TCRN0000059153: CCGGGTGGAACGAATCTACCCATTACTCGAGTAATGGGTAGATTCGTTCCACTTTTTG TCRN0000059154: CCGGGCTGAACACCAATGAACGTTTCTCGAGAAACGTTCATTGGTGTTCAGCTTTTTG TCRN0000059155: CCGGCGACTGGTTCGAATGTGAGAACTCGAGTTCTCACATTCGAACCAGTCGTTTTTG TCRN0000059156: CCGGCCACAGTTGCTTTGAGCACATCTCGAGATGTGCTCAAAGCAACTGTGGTTTTTG TCRN0000059157: CCGGGCTAAACTGCACGGTCAAGAACTCGAGTTCTTGACCGTGCAGTTTAGCTTTTTG) and nontargeting control shRNA (SHC002) were purchased from Mission Sigma-Aldrich. Lentiviral clones overexpressing IL-17A (RC218057) and control vector (pCMV6) were purchased from OriGene. Using Lipofectamine 2000 (Invitrogen), viral particles were produced in 293T cells with PAX2 and VSVG helper plasmids (Addgene). Media on the 293T cells was changed 18 h after transfection with stem cell medium, and, 1 d later, viral supernatants were collected, filtered, and used or frozen at −80°C.

Statistical analysis. Statistical significance was calculated with GraphPad Prism Software using a 1-way or 2-way ANOVA with a Bonferroni's post-test, Student's *t* test, or log-rank (Mantel-Cox) test where appropriate (GraphPad Software Inc.). Data are represented as the mean ± SD.

The study was supported by the International Fellowship Grant of American Society of Colon and Rectal Surgeons (to A.M. Jarrar); Italy-USA Onco-Proteomic Research Program (to F. Lotti); CA154130, CA129958 (to J.N. Rich); CA151522 (to A.B. Hjelmeland); NS063057 (to M. Hitomi and A. Vasanji); National Institutes of Health K99/R00 CA157948, V Scholar Award from the V Foundation for Cancer Research (to J. Lathia); T32 GM007250, F30 CA165857 (to K. Sukhdeo). M.F. Kalady is the Krause-Lieberman Chair in Colorectal Surgery.

The authors have no conflicting financial interests.

Author contributions. Conception and design: F. Lotti, A. Jarrar, A.B. Hjelmeland, M.F. Kalady, J.N. Rich. Development of methodology: F. Lotti, A.M. Jarrar, R.K. Pai, M. Hitomi, J. Lathia, K. Sukhdeo; acquisition of data (provided animals, acquired and managed patients, provided facilities, etc.): F. Lotti, A.M. Jarrar, R.K. Pai, M. Hitomi, J. Lathia, A. Mace, G.A. Gantt Jr., K. Sukhdeo, J. DeVecchio, A. Vasanji, P. Leahy, M.F. Kalady, J.N. Rich; analysis and interpretation of data (e.g., statistical analysis, biostatistics, computational analysis): F. Lotti, A.M. Jarrar, R.K. Pai, M. Hitomi, J. Lathia, G.A. Gantt Jr., J. DeVecchio, A. Vasanji, P. Leahy, M.F. Kalady, J.N. Rich; writing, review, and/or revision of the manuscript: F. Lotti, A. Jarrar, J. Lathia, A.B. Hjelmeland, M.F. Kalady, J.N. Rich; administrative, technical, or material support (i.e., reporting or organizing data, constructing database): F. Lotti, A.M. Jarrar, M. Hitomi, A. Mace, G.A. Gantt Jr., K. Sukhdeo, A. Vasanji, P. Leahy, A.B. Hjelmeland, M.F. Kalady, J.N. Rich; study supervision: M.F. Kalady, J.N. Rich; designed and conducted experiments: F. Lotti, A.M. Jarrar, M. Hitomi, A.B. Hjelmeland, M.F. Kalady, J.N. Rich.

Submitted: Submitted: 6 June 2013
Accepted: Accepted: 21 November 2013

REFERENCES

Acharyya, S., T. Oskarsson, S. Vanharanta, S. Malladi, J. Kim, P.G. Morris, K. Manova-Todorova, M. Leversha, N. Hogg, V.E. Seshan, et al. 2012. A CXCL1 paracrine network links cancer chemoresistance and metastasis. *Cell*. 150:165–178. http://dx.doi.org/10.1016/j.cell.2012.04.042

Allinen, M., R. Beroukhim, L. Cai, C. Brennan, J. Lahti-Domenici, H. Huang, D. Porter, M. Hu, L. Chin, A. Richardson, et al. 2004. Molecular characterization of the tumor microenvironment in breast cancer. *Cancer Cell*. 6:17–32. http://dx.doi.org/10.1016/j.ccr.2004.06.010

American Cancer Society. 2011. American Cancer Society. Colorectal Cancer Facts & Figures 2011-2013. http://www.cancer.org/research/cancerfactsstatistics/colorectal-cancer-facts-figures

Arnold, D., and T. Seufferlein. 2010. Targeted treatments in colorectal cancer: state of the art and future perspectives. *Gut*. 59:838–858. http://dx.doi.org/10.1136/gut.2009.196006

Barcellos-Hoff, M.H., and S.A. Ravani. 2000. Irradiated mammary gland stroma promotes the expression of tumorigenic potential by unirradiated epithelial cells. *Cancer Res.* 60:1254–1260.

Barker, N., J.H. van Es, J. Kuipers, P. Kujala, M. van den Born, M. Cozijnsen, A. Haegebarth, J. Korving, H. Begthel, P.J. Peters, and H. Clevers. 2007. Identification of stem cells in small intestine and colon by marker gene Lgr5. *Nature*. 449:1003–1007. http://dx.doi.org/10.1038/nature06196

Barker, N., R.A. Ridgway, J.H. van Es, M. van de Wetering, H. Begthel, M. van den Born, E. Danenberg, A.R. Clarke, O.J. Sansom, and H. Clevers. 2009. Crypt stem cells as the cells-of-origin of intestinal cancer. *Nature*. 457:608–611. http://dx.doi.org/10.1038/nature07602

Bissell, M.J., and M.A. Labarge. 2005. Context, tissue plasticity, and cancer: are tumor stem cells also regulated by the microenvironment? *Cancer Cell*. 7:17–23.

Blache, P., M. van de Wetering, I. Duluc, C. Domon, P. Berta, J.N. Freund, H. Clevers, and P. Jay. 2004. SOX9 is an intestine crypt transcription factor, is regulated by the Wnt pathway, and represses the CDX2 and MUC2 genes. *J. Cell Biol.* 166:37–47. http://dx.doi.org/10.1083/jcb.200311021

Blanpain, C. 2013. Tracing the cellular origin of cancer. *Nat. Cell Biol.* 15:126–134. http://dx.doi.org/10.1038/ncb2657

Bonnet, D., and J.E. Dick. 1997. Human acute myeloid leukemia is organized as a hierarchy that originates from a primitive hematopoietic cell. *Nat. Med.* 3:730–737. http://dx.doi.org/10.1038/nm0797-730

Bruchard, M., G. Mignot, V. Derangère, F. Chalmin, A. Chevriaux, F. Végran, W. Boireau, B. Simon, B. Ryffel, J.L. Connat, et al. 2013. Chemotherapy-triggered cathepsin B release in myeloid-derived suppressor cells activates the Nlrp3 inflammasome and promotes tumor growth. *Nat. Med.* 19:57–64. http://dx.doi.org/10.1038/nm.2999

Calon, A., E. Espinet, S. Palomo-Ponce, D.V. Tauriello, M. Iglesias, M.V. Céspedes, M. Sevillano, C. Nadal, P. Jung, X.H. Zhang, et al. 2012. Dependency of colorectal cancer on a TGF-β-driven program in stromal cells for metastasis initiation. *Cancer Cell*. 22:571–584. http://dx.doi.org/10.1016/j.ccr.2012.08.013

Chung, A.S., X. Wu, G. Zhuang, H. Ngu, I. Kasman, J. Zhang, J.M. Vernes, Z. Jiang, Y.G. Meng, F.V. Peale, et al. 2013. An interleukin-17-mediated paracrine network promotes tumor resistance to anti-angiogenic therapy. *Nat. Med.* 19:1114–1123. http://dx.doi.org/10.1038/nm.3291

Crawford, Y., I. Kasman, L. Yu, C. Zhong, X. Wu, Z. Modrusan, J. Kaminker, and N. Ferrara. 2009. PDGF-C mediates the angiogenic and tumorigenic properties of fibroblasts associated with tumors refractory to anti-VEGF treatment. *Cancer Cell*. 15:21–34. http://dx.doi.org/10.1016/j.ccr.2008.12.004

Dalerba, P., S.J. Dylla, I.K. Park, R. Liu, X. Wang, R.W. Cho, T. Hoey, A. Gurney, E.H. Huang, D.M. Simeone, et al. 2007. Phenotypic characterization of human colorectal cancer stem cells. *Proc. Natl. Acad. Sci. USA*. 104:10158–10163. http://dx.doi.org/10.1073/pnas.0703478104

Dallas, N.A., L. Xia, F. Fan, M.J. Gray, P. Gaur, G. van Buren II, S. Samuel, M.P. Kim, S.J. Lim, and L.M. Ellis. 2009. Chemoresistant colorectal cancer cells, the cancer stem cell phenotype, and increased sensitivity to insulin-like growth factor-I receptor inhibition. *Cancer Res.* 69:1951–1957. http://dx.doi.org/10.1158/0008-5472.CAN-08-2023

De Wever, O., and M. Mareel. 2002. Role of myofibroblasts at the invasion front. *Biol. Chem.* 383:55–67. http://dx.doi.org/10.1515/BC.2002.006

Deng, S., X. Yang, H. Lassus, S. Liang, S. Kaur, Q. Ye, C. Li, L.P. Wang, K.F. Roby, S. Orsulic, et al. 2010. Distinct expression levels and patterns of stem cell marker, aldehyde dehydrogenase isoform 1 (ALDH1), in human epithelial cancers. *PLoS ONE*. 5:e10277. http://dx.doi.org/10.1371/journal.pone.0010277

Desmoulière, A., C. Guyot, and G. Gabbiani. 2004. The stroma reaction myofibroblast: a key player in the control of tumor cell behavior. *Int. J. Dev. Biol.* 48:509–517. http://dx.doi.org/10.1387/ijdb.041802ad

Du, L., H. Wang, L. He, J. Zhang, B. Ni, X. Wang, H. Jin, N. Cahuzac, M. Mehrpour, Y. Lu, and Q. Chen. 2008. CD44 is of functional importance for colorectal cancer stem cells. *Clin. Cancer Res.* 14:6751–6760. http://dx.doi.org/10.1158/1078-0432.CCR-08-1034

Dvorak, H.F. 1986. Tumors: wounds that do not heal. Similarities between tumor stroma generation and wound healing. *N. Engl. J. Med.* 315:1650–1659. http://dx.doi.org/10.1056/NEJM198612253152606

Dylla, S.J., L. Beviglia, I.K. Park, C. Chartier, J. Raval, L. Ngan, K. Pickell, J. Aguilar, S. Lazetic, S. Smith-Berdan, et al. 2008. Colorectal cancer stem cells are enriched in xenogeneic tumors following chemotherapy. *PLoS ONE*. 3:e2428. http://dx.doi.org/10.1371/journal.pone.0002428

Edge, S., D. Byrd, M. Carducci, and C. Compton. 2009. AJCC Cancer Staging Manual. Springer, New York.

Elsaba, T.M., L. Martinez-Pomares, A.R. Robins, S. Crook, R. Seth, D. Jackson, A. McCart, A.R. Silver, I.P. Tomlinson, and M. Ilyas. 2010. The stem cell marker CD133 associates with enhanced colony formation and cell motility in colorectal cancer. *PLoS ONE*. 5:e10714. http://dx.doi.org/10.1371/journal.pone.0010714

Erez, N., M. Truitt, P. Olson, S.T. Arron, and D. Hanahan. 2010. Cancer-Associated Fibroblasts Are Activated in Incipient Neoplasia to Orchestrate Tumor-Promoting Inflammation in an NF-kappaB-Dependent Manner. *Cancer Cell*. 17:135–147. http://dx.doi.org/10.1016/j.ccr.2009.12.041

Fang, D.D., Y.J. Kim, C.N. Lee, S. Aggarwal, K. McKinnon, D. Mesmer, J. Norton, C.E. Birse, T. He, S.M. Ruben, and P.A. Moore. 2010. Expansion of CD133(+) colon cancer cultures retaining stem cell properties to enable cancer stem cell target discovery. *Br. J. Cancer*. 102:1265–1275. http://dx.doi.org/10.1038/sj.bjc.6605610

Gemei, M., P. Mirabelli, R. Di Noto, C. Corbo, A. Iaccarino, A. Zamboli, G. Troncone, G. Galizia, E. Lieto, L. Del Vecchio, and F. Salvatore. 2013. CD66c is a novel marker for colorectal cancer stem cell isolation, and its silencing halts tumor growth in vivo. *Cancer*. 119:729–738. http://dx.doi.org/10.1002/cncr.27794

Gilbert, L.A., and M.T. Hemann. 2010. DNA damage-mediated induction of a chemoresistant niche. *Cell*. 143:355–366. http://dx.doi.org/10.1016/j.cell.2010.09.043

Gilbert, L.A., and M.T. Hemann. 2011. Chemotherapeutic resistance: surviving stressful situations. *Cancer Res.* 71:5062–5066. http://dx.doi.org/10.1158/0008-5472.CAN-11-0277

Gonda, T.A., A. Varro, T.C. Wang, and B. Tycko. 2010. Molecular biology of cancer-associated fibroblasts: can these cells be targeted in anticancer therapy? *Semin. Cell Dev. Biol.* 21:2–10. http://dx.doi.org/10.1016/j.semcdb.2009.10.001

Grivennikov, S.I., K. Wang, D. Mucida, C.A. Stewart, B. Schnabl, D. Jauch, K. Taniguchi, G.Y. Yu, C.H. Osterreicher, K.E. Hung, et al. 2012. Adenoma-linked barrier defects and microbial products drive IL-23/IL-17-mediated tumour growth. *Nature*. 491:254–258.

Grum-Schwensen, B., J. Klingelhofer, C.H. Berg, C. El-Naaman, M. Grigorian, E. Lukanidin, and N. Ambartsumian. 2005. Suppression of tumor development and metastasis formation in mice lacking the S100A4(mts1) gene. *Cancer Res.* 65:3772–3780. http://dx.doi.org/10.1158/0008-5472.CAN-04-4510

Guo, W., Z. Keckesova, J.L. Donaher, T. Shibue, V. Tischler, F. Reinhardt, S. Itzkovitz, A. Noske, U. Zürrer-Härdi, G. Bell, et al. 2012. Slug and Sox9 cooperatively determine the mammary stem cell state. *Cell*. 148:1015–1028. http://dx.doi.org/10.1016/j.cell.2012.02.008

Hao, M., L. Zhang, G. An, H. Meng, Y. Han, Z. Xie, Y. Xu, C. Li, Z. Yu, H. Chang, and L. Qiu. 2011. Bone marrow stromal cells protect myeloma cells from bortezomib induced apoptosis by suppressing microRNA-15a expression. *Leuk. Lymphoma*. 52:1787–1794. http://dx.doi.org/10.3109/10428194.2011.576791

Hellevik, T., I. Pettersen, V. Berg, J. Bruun, K. Bartnes, L.T. Busund, A. Chalmers, R. Bremnes, and I. Martinez-Zubiaurre. 2013. Changes in the Secretory Profile of NSCLC-Associated Fibroblasts after Ablative Radiotherapy: Potential Impact on Angiogenesis and Tumor Growth. *Transl Oncol*. 6:66–74.

Hölzel, M., A. Bovier, and T. Tüting. 2013. Plasticity of tumour and immune cells: a source of heterogeneity and a cause for therapy resistance? *Nat. Rev. Cancer*. 13:365–376. http://dx.doi.org/10.1038/nrc3498

Horst, D., L. Kriegl, J. Engel, T. Kirchner, and A. Jung. 2009. Prognostic significance of the cancer stem cell markers CD133, CD44, and CD166 in colorectal cancer. *Cancer Invest*. 27:844–850. http://dx.doi.org/10.1080/07357900902744502

Hu, Y., and G.K. Smyth. 2009. ELDA: extreme limiting dilution analysis for comparing depleted and enriched populations in stem cell and other assays. *J. Immunol. Methods*. 347:70–78. http://dx.doi.org/10.1016/j.jim.2009.06.008

Huang, E.H., M.J. Hynes, T. Zhang, C. Ginestier, G. Dontu, H. Appelman, J.Z. Fields, M.S. Wicha, and B.M. Boman. 2009. Aldehyde dehydrogenase 1 is a marker for normal and malignant human colonic stem cells (SC) and tracks SC overpopulation during colon tumorigenesis. *Cancer Res.* 69:3382–3389. http://dx.doi.org/10.1158/0008-5472.CAN-08-4418

Hueber, W., D.D. Patel, T. Dryja, A.M. Wright, I. Koroleva, G. Bruin, C. Antoni, Z. Draelos, M.H. Gold, P. Durez, et al; Psoriasis Study Group; Rheumatoid Arthritis Study Group; Uveitis Study Group. 2010. Effects of AIN457, a fully human antibody to interleukin-17A, on psoriasis, rheumatoid arthritis, and uveitis. *Sci. Transl. Med.* 2:52ra72. http://dx.doi.org/10.1126/scitranslmed.3001107

Hyun, Y.S., D.S. Han, A.R. Lee, C.S. Eun, J. Youn, and H.Y. Kim. 2012. Role of IL-17A in the development of colitis-associated cancer. *Carcinogenesis.* 33:931–936. http://dx.doi.org/10.1093/carcin/bgs106

Jay, P., P. Berta, and P. Blache. 2005. Expression of the carcinoembryonic antigen gene is inhibited by SOX9 in human colon carcinoma cells. *Cancer Res.* 65:2193–2198. http://dx.doi.org/10.1158/0008-5472.CAN-04-1484

Lakshman, M., V. Subramaniam, U. Rubenthiran, and S. Jothy. 2004. CD44 promotes resistance to apoptosis in human colon cancer cells. *Exp. Mol. Pathol.* 77:18–25. http://dx.doi.org/10.1016/j.yexmp.2004.03.002

Lakshman, M., V. Subramaniam, S. Wong, and S. Jothy. 2005. CD44 promotes resistance to apoptosis in murine colonic epithelium. *J. Cell. Physiol.* 203:583–588. http://dx.doi.org/10.1002/jcp.20260

Leonardi, C., R. Matheson, C. Zachariae, G. Cameron, L. Li, E. Edson-Heredia, D. Braun, and S. Banerjee. 2012. Anti-interleukin-17 monoclonal antibody ixekizumab in chronic plaque psoriasis. *N. Engl. J. Med.* 366:1190–1199. http://dx.doi.org/10.1056/NEJMoa1109997

Li, H.J., F. Reinhardt, H.R. Herschman, and R.A. Weinberg. 2012. Cancer-stimulated mesenchymal stem cells create a carcinoma stem cell niche via prostaglandin E2 signaling. *Cancer Discov.* 2:840–855. http://dx.doi.org/10.1158/2159-8290.CD-12-0101

Lieubeau, B., L. Garrigue, I. Barbieux, K. Meflah, and M. Gregoire. 1994. The role of transforming growth factor beta 1 in the fibroblastic reaction associated with rat colorectal tumor development. *Cancer Res.* 54:6526–6532.

Liu, S., C. Ginestier, S.J. Ou, S.G. Clouthier, S.H. Patel, F. Monville, H. Korkaya, A. Heath, J. Dutcher, C.G. Kleer, et al. 2011. Breast cancer stem cells are regulated by mesenchymal stem cells through cytokine networks. *Cancer Res.* 71:614–624. http://dx.doi.org/10.1158/0008-5472.CAN-10-0538

Lu, J., X. Ye, F. Fan, L. Xia, R. Bhattacharya, S. Bellister, F. Tozzi, E. Sceusi, Y. Zhou, I. Tachibana, et al. 2013. Endothelial cells promote the colorectal cancer stem cell phenotype through a soluble form of Jagged-1. *Cancer Cell.* 23:171–185. http://dx.doi.org/10.1016/j.ccr.2012.12.021

Magee, J.A., E. Piskounova, and S.J. Morrison. 2012. Cancer stem cells: impact, heterogeneity, and uncertainty. *Cancer Cell.* 21:283–296. http://dx.doi.org/10.1016/j.ccr.2012.03.003

Markowitz, S.D., and M.M. Bertagnolli. 2009. Molecular origins of cancer: Molecular basis of colorectal cancer. *N. Engl. J. Med.* 361:2449–2460. http://dx.doi.org/10.1056/NEJMra0804588

Markowitz, S., J. Wang, L. Myeroff, R. Parsons, L. Sun, J. Lutterbaugh, R.S. Fan, E. Zborowska, K.W. Kinzler, B. Vogelstein, et al. 1995. Inactivation of the type II TGF-beta receptor in colon cancer cells with microsatellite instability. *Science.* 268:1336–1338. http://dx.doi.org/10.1126/science.7761852

Matsunaga, T., N. Takemoto, T. Sato, R. Takimoto, I. Tanaka, A. Fujimi, T. Akiyama, H. Kuroda, Y. Kawano, M. Kobune, et al. 2003. Interaction between leukemic-cell VLA-4 and stromal fibronectin is a decisive factor for minimal residual disease of acute myelogenous leukemia. *Nat. Med.* 9:1158–1165. http://dx.doi.org/10.1038/nm909

Medema, J.P., and L. Vermeulen. 2011. Microenvironmental regulation of stem cells in intestinal homeostasis and cancer. *Nature.* 474:318–326. http://dx.doi.org/10.1038/nature10212

Medzhitov, R., and T. Horng. 2009. Transcriptional control of the inflammatory response. *Nat. Rev. Immunol.* 9:692–703. http://dx.doi.org/10.1038/nri2634

Micke, P., and A. Ostman. 2004. Tumour-stroma interaction: cancer-associated fibroblasts as novel targets in anti-cancer therapy? *Lung Cancer.* 45(Suppl 2): S163–S175. http://dx.doi.org/10.1016/j.lungcan.2004.07.977

Nakasone, E.S., H.A. Askautrud, T. Kees, J.H. Park, V. Plaks, A.J. Ewald, M. Fein, M.G. Rasch, Y.X. Tan, J. Qiu, et al. 2012. Imaging tumor-stroma interactions during chemotherapy reveals contributions of the microenvironment to resistance. *Cancer Cell.* 21:488–503. http://dx.doi.org/10.1016/j.ccr.2012.02.017

Nakayama, H., H. Enzan, E. Miyazaki, and M. Toi. 2002. Alpha smooth muscle actin positive stromal cells in gastric carcinoma. *J. Clin. Pathol.* 55:741–744. http://dx.doi.org/10.1136/jcp.55.10.741

O'Brien, C.A., A. Pollett, S. Gallinger, and J.E. Dick. 2007. A human colon cancer cell capable of initiating tumour growth in immunodeficient mice. *Nature.* 445:106–110. http://dx.doi.org/10.1038/nature05372

Ogino, S., C.S. Fuchs, and E. Giovannucci. 2012. How many molecular subtypes? Implications of the unique tumor principle in personalized medicine. *Expert Rev. Mol. Diagn.* 12:621–628. http://dx.doi.org/10.1586/erm.12.46

Ohata, H., T. Ishiguro, Y. Aihara, A. Sato, H. Sakai, S. Sekine, H. Taniguchi, T. Akasu, S. Fujita, H. Nakagama, and K. Okamoto. 2012. Induction of the stem-like cell regulator CD44 by Rho kinase inhibition contributes to the maintenance of colon cancer-initiating cells. *Cancer Res.* 72:5101–5110. http://dx.doi.org/10.1158/0008-5472.CAN-11-3812

Olumi, A.F., G.D. Grossfeld, S.W. Hayward, P.R. Carroll, T.D. Tlsty, and G.R. Cunha. 1999. Carcinoma-associated fibroblasts direct tumor progression of initiated human prostatic epithelium. *Cancer Res.* 59:5002–5011.

Orimo, A., and R.A. Weinberg. 2007. Heterogeneity of stromal fibroblasts in tumors. *Cancer Biol. Ther.* 6:618–619.

Orimo, A., P.B. Gupta, D.C. Sgroi, F. Arenzana-Seisdedos, T. Delaunay, R. Naeem, V.J. Carey, A.L. Richardson, and R.A. Weinberg. 2005. Stromal fibroblasts present in invasive human breast carcinomas promote tumor growth and angiogenesis through elevated SDF-1/CXCL12 secretion. *Cell.* 121:335–348. http://dx.doi.org/10.1016/j.cell.2005.02.034

Papp, K.A., C. Leonardi, A. Menter, J.P. Ortonne, J.G. Krueger, G. Kricorian, G. Aras, J. Li, C.B. Russell, E.H. Thompson, and S. Baumgartner. 2012. Brodalumab, an anti-interleukin-17-receptor antibody for psoriasis. *N. Engl. J. Med.* 366:1181–1189. http://dx.doi.org/10.1056/NEJMoa1109017

Park, J.E., M.C. Lenter, R.N. Zimmermann, P. Garin-Chesa, L.J. Old, and W.J. Rettig. 1999. Fibroblast activation protein, a dual specificity serine protease expressed in reactive human tumor stromal fibroblasts. *J. Biol. Chem.* 274:36505–36512. http://dx.doi.org/10.1074/jbc.274.51.36505

Park, J.J., J.H. Kwon, S.H. Oh, J. Choi, C.M. Moon, J.B. Ahn, S.P. Hong, J.H. Cheon, T.I. Kim, H. Kim, and W.H. Kim. 2012. Differential expression of CD133 based on microsatellite instability status in human colorectal cancer. *Mol. Carcinog.* 10.1002/mc.21971.

Peñuelas, S., J. Anido, R.M. Prieto-Sánchez, G. Folch, I. Barba, I. Cuartas, D. García-Dorado, M.A. Poca, J. Sahuquillo, J. Baselga, and J. Seoane. 2009. TGF-beta increases glioma-initiating cell self-renewal through the induction of LIF in human glioblastoma. *Cancer Cell.* 15:315–327. http://dx.doi.org/10.1016/j.ccr.2009.02.011

Porter, D.C., E. Farmaki, S. Altilia, G.P. Schools, D.K. West, M. Chen, B.D. Chang, A.T. Puzyrev, C.U. Lim, R. Rokow-Kittell, et al. 2012. Cyclin-dependent kinase 8 mediates chemotherapy-induced tumor-promoting paracrine activities. *Proc. Natl. Acad. Sci. USA.* 109:13799–13804. http://dx.doi.org/10.1073/pnas.1206906109

Ricci-Vitiani, L., D.G. Lombardi, E. Pilozzi, M. Biffoni, M. Todaro, C. Peschle, and R. De Maria. 2007. Identification and expansion of human colon-cancer-initiating cells. *Nature.* 445:111–115. http://dx.doi.org/10.1038/nature05384

Ricci-Vitiani, L., E. Fabrizi, E. Palio, and R. De Maria. 2009. Colon cancer stem cells. *J. Mol. Med.* 87:1097–1104. http://dx.doi.org/10.1007/s00109-009-0518-4

Rønnov-Jessen, L., O.W. Petersen, and M.J. Bissell. 1996. Cellular changes involved in conversion of normal to malignant breast: importance of the stromal reaction. *Physiol. Rev.* 76:69–125.

Sadanandam, A., C.A. Lyssiotis, K. Homicsko, E.A. Collisson, W.J. Gibb, S. Wullschleger, L.C. Ostos, W.A. Lannon, C. Grotzinger, M. Del Rio, et al. 2013. A colorectal cancer classification system that associates

cellular phenotype and responses to therapy. *Nat. Med.* 19:619–625. http://dx.doi.org/10.1038/nm.3175

Sanchez, J.A., L. Krumroy, S. Plummer, P. Aung, A. Merkulova, M. Skacel, K.L. DeJulius, E. Manilich, J.M. Church, G. Casey, and M.F. Kalady. 2009. Genetic and epigenetic classifications define clinical phenotypes and determine patient outcomes in colorectal cancer. *Br. J. Surg.* 96:1196–1204. http://dx.doi.org/10.1002/bjs.6683

Sappino, A.P., O. Skalli, B. Jackson, W. Schürch, and G. Gabbiani. 1988. Smooth-muscle differentiation in stromal cells of malignant and non-malignant breast tissues. *Int. J. Cancer.* 41:707–712. http://dx.doi.org/10.1002/ijc.2910410512

Sato, T., J.H. van Es, H.J. Snippert, D.E. Stange, R.G. Vries, M. van den Born, N. Barker, N.F. Shroyer, M. van de Wetering, and H. Clevers. 2011. Paneth cells constitute the niche for Lgr5 stem cells in intestinal crypts. *Nature.* 469:415–418. http://dx.doi.org/10.1038/nature09637

Schäfer, M., and S. Werner. 2008. Cancer as an overhealing wound: an old hypothesis revisited. *Nat. Rev. Mol. Cell Biol.* 9:628–638. http://dx.doi.org/10.1038/nrm2455

Schuijers, J., and H. Clevers. 2012. Adult mammalian stem cells: the role of Wnt, Lgr5 and R-spondins. *EMBO J.* 31:2685–2696. http://dx.doi.org/10.1038/emboj.2012.149

Schwitalla, S., A.A. Fingerle, P. Cammareri, T. Nebelsiek, S.I. Göktuna, P.K. Ziegler, O. Canli, J. Heijmans, D.J. Huels, G. Moreaux, et al. 2013. Intestinal tumorigenesis initiated by dedifferentiation and acquisition of stem-cell-like properties. *Cell.* 152:25–38. http://dx.doi.org/10.1016/j.cell.2012.12.012

Serini, G., and G. Gabbiani. 1999. Mechanisms of myofibroblast activity and phenotypic modulation. *Exp. Cell Res.* 250:273–283. http://dx.doi.org/10.1006/excr.1999.4543

Shaked, Y., A. Ciarrocchi, M. Franco, C.R. Lee, S. Man, A.M. Cheung, D.J. Hicklin, D. Chaplin, F.S. Foster, R. Benezra, and R.S. Kerbel. 2006. Therapy-induced acute recruitment of circulating endothelial progenitor cells to tumors. *Science.* 313:1785–1787. http://dx.doi.org/10.1126/science.1127592

Shaked, Y., E. Henke, J.M. Roodhart, P. Mancuso, M.H. Langenberg, M. Colleoni, L.G. Daenen, S. Man, P. Xu, U. Emmenegger, et al. 2008. Rapid chemotherapy-induced acute endothelial progenitor cell mobilization: implications for antiangiogenic drugs as chemosensitizing agents. *Cancer Cell.* 14:263–273. http://dx.doi.org/10.1016/j.ccr.2008.08.001

Shmelkov, S.V., J.M. Butler, A.T. Hooper, A. Hormigo, J. Kushner, T. Milde, R. St Clair, M. Baljevic, I. White, D.K. Jin, et al. 2008. CD133 expression is not restricted to stem cells, and both CD133+ and CD133- metastatic colon cancer cells initiate tumors. *J. Clin. Invest.* 118:2111–2120.

Shree, T., O.C. Olson, B.T. Elie, J.C. Kester, A.L. Garfall, K. Simpson, K.M. Bell-McGuinn, E.C. Zabor, E. Brogi, and J.A. Joyce. 2011. Macrophages and cathepsin proteases blunt chemotherapeutic response in breast cancer. *Genes Dev.* 25:2465–2479. http://dx.doi.org/10.1101/gad.180331.111

Straussman, R., T. Morikawa, K. Shee, M. Barzily-Rokni, Z.R. Qian, J. Du, A. Davis, M.M. Mongare, J. Gould, D.T. Frederick, et al. 2012. Tumour micro-environment elicits innate resistance to RAF inhibitors through HGF secretion. *Nature.* 487:500–504. http://dx.doi.org/10.1038/nature11183

Sugimoto, H., T.M. Mundel, M.W. Kieran, and R. Kalluri. 2006. Identification of fibroblast heterogeneity in the tumor microenvironment. *Cancer Biol. Ther.* 5:1640–1646. http://dx.doi.org/10.4161/cbt.5.12.3354

Takahashi, K., and S. Yamanaka. 2006. Induction of pluripotent stem cells from mouse embryonic and adult fibroblast cultures by defined factors. *Cell.* 126:663–676. http://dx.doi.org/10.1016/j.cell.2006.07.024

Takahashi, H., H. Ishii, N. Nishida, I. Takemasa, T. Mizushima, M. Ikeda, T. Yokobori, K. Mimori, H. Yamamoto, M. Sekimoto, et al. 2011. Significance of Lgr5(+ve) cancer stem cells in the colon and rectum. *Ann. Surg. Oncol.* 18:1166–1174. http://dx.doi.org/10.1245/s10434-010-1373-9

Todaro, M., M.P. Alea, A.B. Di Stefano, P. Cammareri, L. Vermeulen, F. Iovino, C. Tripodo, A. Russo, G. Gulotta, J.P. Medema, and G. Stassi. 2007. Colon cancer stem cells dictate tumor growth and resist cell death by production of interleukin-4. *Cell Stem Cell.* 1:389–402. http://dx.doi.org/10.1016/j.stem.2007.08.001

Tuxhorn, J.A., S.J. McAlhany, F. Yang, T.D. Dang, and D.R. Rowley. 2002. Inhibition of transforming growth factor-beta activity decreases angiogenesis in a human prostate cancer-reactive stroma xenograft model. *Cancer Res.* 62:6021–6025.

Vermeulen, L., M. Todaro, F. de Sousa Mello, M.R. Sprick, K. Kemper, M. Perez Alea, D.J. Richel, G. Stassi, and J.P. Medema. 2008. Single-cell cloning of colon cancer stem cells reveals a multi-lineage differentiation capacity. *Proc. Natl. Acad. Sci. USA.* 105:13427–13432. http://dx.doi.org/10.1073/pnas.0805706105

Vermeulen, L., F. De Sousa E Melo, M. van der Heijden, K. Cameron, J.H. de Jong, T. Borovski, J.B. Tuynman, M. Todaro, C. Merz, H. Rodermond, et al. 2010. Wnt activity defines colon cancer stem cells and is regulated by the microenvironment. *Nat. Cell Biol.* 12:468–476. http://dx.doi.org/10.1038/ncb2048

Wang, H., J.D. Lathia, Q. Wu, J. Wang, Z. Li, J.M. Heddleston, C.E. Eyler, J. Elderbroom, J. Gallagher, J. Schuschu, et al. 2009. Targeting interleukin 6 signaling suppresses glioma stem cell survival and tumor growth. *Stem Cells.* 27:2393–2404. http://dx.doi.org/10.1002/stem.188

Washington, M.K., J. Berlin, P. Branton, L.J. Burgart, D.K. Carter, P.L. Fitzgibbons, K. Halling, W. Frankel, J. Jessup, S. Kakar, et al; Members of the Cancer Committee, College of American Pathologists. 2009. Protocol for the examination of specimens from patients with primary carcinoma of the colon and rectum. *Arch. Pathol. Lab. Med.* 133:1539–1551.

Weaver, V.M., S. Lelièvre, J.N. Lakins, M.A. Chrenek, J.C. Jones, F. Giancotti, Z. Werb, and M.J. Bissell. 2002. beta4 integrin-dependent formation of polarized three-dimensional architecture confers resistance to apoptosis in normal and malignant mammary epithelium. *Cancer Cell.* 2:205–216. http://dx.doi.org/10.1016/S1535-6108(02)00125-3

Winder, T., and H.J. Lenz. 2010. Vascular endothelial growth factor and epidermal growth factor signaling pathways as therapeutic targets for colorectal cancer. *Gastroenterology.* 138:2163–2176. http://dx.doi.org/10.1053/j.gastro.2010.02.005

Worthley, D.L., A.S. Giraud, and T.C. Wang. 2010. Stromal fibroblasts in digestive cancer. *Cancer Microenviron.* 3:117–125. http://dx.doi.org/10.1007/s12307-009-0033-8

Wu, S., K.J. Rhee, E. Albesiano, S. Rabizadeh, X. Wu, H.R. Yen, D.L. Huso, F.L. Brancati, E. Wick, F. McAllister, et al. 2009. A human colonic commensal promotes colon tumorigenesis via activation of T helper type 17 T cell responses. *Nat. Med.* 15:1016–1022. http://dx.doi.org/10.1038/nm.2015

Xing, F., J. Saidou, and K. Watabe. 2010. Cancer associated fibroblasts (CAFs) in tumor microenvironment. *Front Biosci (Landmark Ed).* 15:166–179. http://dx.doi.org/10.2741/3613

Yamauchi, K., M. Yang, K. Hayashi, P. Jiang, N. Yamamoto, H. Tsuchiya, K. Tomita, A.R. Moossa, M. Bouvet, and R.M. Hoffman. 2008. Induction of cancer metastasis by cyclophosphamide pretreatment of host mice: an opposite effect of chemotherapy. *Cancer Res.* 68:516–520. http://dx.doi.org/10.1158/0008-5472.CAN-07-3063

Yeung, T.M., S.C. Gandhi, J.L. Wilding, R. Muschel, and W.F. Bodmer. 2010. Cancer stem cells from colorectal cancer-derived cell lines. *Proc. Natl. Acad. Sci. USA.* 107:3722–3727. http://dx.doi.org/10.1073/pnas.0915135107